Addis Ababa University

College of Social Sciences

Department of Geography and Environmental Studies

Program: GIS, Remote Sensing and Digital Cartography

Performance Evaluation of Satellite Rainfall Estimates for Flood Monitoring in *Gumera* Watershed, Amhara Region, Ethiopia

By

Gebrie Tsegaye Mersha

December, 2022

Addis Ababa, Ethiopia

Performance Evaluation of Satellite Rainfall Estimates for Flood Monitoring in *Gumera* Watershed, Amhara Region, Ethiopia

Gebrie Tsegaye Mersha

A Thesis Submitted to

The Department of Geography and Environmental Studies Presented in Partial Fulfillment of the Requirements for the degree of Master of Arts (GIS, Remote Sensing and Digital Cartography)

Advisor: Asnake Mekuriaw (Ph.D.)

Addis Ababa University
Addis Ababa, Ethiopia
December, 2022

DECLARATION

I, the undersigned confirm that the thesis is my own work. I have recognized and cited all sources used in this work in accordance with generally accepted standards of practice. I am aware that failure to uphold the standards of academic honesty and integrity, as well as the misrepresentation or fabrication of any idea, data, fact, or source, will be grounds for discipline by the university as well as legal action from sources who have not been properly acknowledged or cited.

Gebrie Tsegaye Mersha

Signature: ________________

Date: ___________________

ADDIS ABABA UNIVERSITY

COLLEGE OF SOCIAL SCIENCES

DEPARTMENT OF GEOGRAPHY AND ENVIRONMENTAL STUDIES

APPROVAL SHEET

This is to certify that the thesis prepared by Gebrie Tsegaye Mersha entitled: *Performance Evaluation of Satellite Rainfall Estimates for Flood Monitoring in Gumera Watershed, Amhara Region, Ethiopia* is submitted in partial fulfillment of the Requirements for the Degree of Master of Arts (GIS, Remote Sensing and Digital Cartography) complies with the regulation of the University and meets the accepted standards with respect to originality and quality.

Signed by the Examining Committee:

Advisor: Asnake Mekuriaw (Ph.D.) Signature _________ Date ___________

Internal Examiner: ______________________ Signature _________ Date _________

External Examiner: ______________________ Signature _________ Date ________

____

Chair of Department or Graduate Program Coordinator

Abstract

Since the 1980s, several satellites have been providing rainfall data for the tropical parts of the world, including Ethiopia. These data could be used for different applications in various fields of study in areas where ground-based rain gauge stations are unavailable and sparsely distributed. The purpose of this study is to evaluate the performances of satellite rainfall estimates (CHIRPS-V2, TAMSAT-V3.1, and PERSIANN-CDR) for flood monitoring in the most flood-prone area of Amhara Region, Ethiopia. Daily rainfall data from 2004 to 2019 were collected from the National Meteorological Agency. In Addition, satellite rainfall estimates that cover the same periods, and historical flood events in the study area were collected from the internet database and district agriculture office respectively. Continuous statistical indices and categorical statistical indices were employed for data analysis. The performances of the three-satellite rainfall estimates were evaluated on four major temporal scales; annual, seasonal, monthly, and daily temporal scale. In terms of annual and seasonal temporal scales, TAMSAT-V3.1 and CHIRPS-V2 performed well and outperformed PERSIANN-CDR on the major statistical indices. In the Monthly temporal scale, CHIRPS-V2 performed well on the major continuous statistical indices. The application of satellite rainfall products for flood monitoring is also evaluated by using the daily rainfall estimates in two ways; using the overall daily observed rainfall from 2004 to 2019 and using the daily rainfall data during the three most flood events (2006, 2017 and 2019) in the study area. In both cases, all the three satellite datasets underestimate the highest amount of observed rainfall and overestimate the lowest amount of daily rainfall conditions. Relatively, CHIRPS-V2 had the best skill in estimating the highest daily rainfall observed in the study area. This research indicated that performance evaluation of satellite rainfall datasets must be conducted before applying for flood monitoring. The study could not address the performance of satellite rainfall estimates in predicting when and where floods will occur in the future. Therefore, future research should be focused on the flood prediction performance of satellite-derived rainfall data.

Keywords: *Remote Sensing; Flood; Satellite rainfall Estimate, Evaluation; dataset*

Acknowledgment

This thesis is the output of a joint effort of so many people, whom I can't mention all here. Yet, my special gratitude and genuine appreciation go to Asnake Mekuriaw (PhD), my research advisor, for his unreserved comments, advice, and intellectual guidance. I would like, to thank the Ethiopian National Meteorological Agency (the current institute) for their welcoming approach during the data collection process. Moreover, I have to acknowledge the **Konrad-Adenauer-Stiftung Foundation Office Ethiopia/African Union,** for financial support during my study period. I owe special gratitude to my beloved wife, Sewnet Demelash, for her support and love for our children, Aklesia and Kidus. Above all, I want to thank the Almighty God for his immeasurable blessings in my life and for his assistance with this study.

Table of Content

Contents **Page**

List of Figures

List of Tables

List of Acronyms

ARC	African Rainfall Estimate Climatology
CCD	Cold Cloud Duration
CDR	Climate Data Records
CHIRPS	Climate Hazards Group InfraRed Precipitation with Stations
CHRS	Center for Hydrometeorology and Remote Sensing
CPC	Climate Prediction Center
CMAP	Climate Prediction Centre (CPC) Merged Analysis of Precipitation
DEM	Digital Elevation Model
GIS	Geographic Information System
GPCP	Global Precipitation Climatology Project
GPM	Global Precipitation Measurement
GSMaP	Global Satellite Mapping of Precipitation
IMERG	Integrated Multi-satellite Retrievals for GPM
NCAS	National Center for Atmospheric Science
NCDC	National Climatic Data Center
NCEO	National Center for Earth Observation
NetCDF	Network Common Data Form
NOAA	National Oceanic and Atmospheric Administration
NMA	National Meteorological Agency
PERSIANN	Precipitation Estimation from Remotely Sensed Information Using Artificial Neural Networks

PERSIANN-CCS	Precipitation Estimation from Remotely Sensed Information Using Artificial Neural Networks Cloud Classification System
PERSIANN-CDR	Precipitation Estimation from Remotely Sensed Information Using Artificial Neural Networks Climate Data Record
SRE	Satellite Rainfall Estimates
TAMSAT	Tropical Applications of Meteorology using Satellite and Ground-based observations
TARCAT	African Rainfall Climatology and Timeseries

Chapter One

1. Introduction

1.1. Background of the Study

The role of Geographic Information System (GIS) and Remote Sensing is immense in the processes of describing, characterizing and analyzing various physical and human aspects of the earth. In recent years, the use of satellite Remote Sensing techniques for the measurement and monitoring of meteorological and associated parameters at the Earth's surface and in the atmosphere has become increasingly important (WMO, 2008). Its goal is to define space-based data in relation to surface-based data systems. Remote sensing and GIS can strengthen the availability of different types of data, including various meteorological elements such as rainfall, temperature, and humidity (Kyaw, 2020).

Rainfall is a crucial meteorological and hydrological element that has a significant impact on agricultural production and the Earth's energy balance (Ayehu et al., 2018; Yu et al., 2020). The water cycle, climate, and earth ecosystems are all influenced by the rate, amount, and distribution of rainfall variability, which has an impact on all elements of human life, including agricultural economics and social activities (Alhamshry et al., 2020). Rainfall is the most important meteorological variable for society's survival in developing countries like Ethiopia, where over 80% of the population relies on rain-fed agriculture (Bewket, 2009; Tote et al., 2015). It is also crucial for the generation of hydropower energy from various dams built on the country's major rivers. The considerable spatial and temporal variability of rainfall, on the other hand, has an impact on every facet of its utilization in agriculture and other parts of the economy (Darand and

Siavashi, 2021). These impacts can be in the form of floods, drought, soil erosion, or others.

In Ethiopia, flood is one of the major environmental problems that affect the lives of the society and their livelihoods (FDRE National Disaster Risk Management Commission, 2018). According to a World Bank report (2019), flood poses the most significant and recurring risk in Ethiopia. The report prevail that flooding poses a threat to urban and rural areas, with 250,000 people affected each year, on average in the country. It also indicated that future changes in Ethiopia's population and economy, coupled with changes in climate-related hazards, are expected to increase the impacts of floods in different regions of the country.

According to OCHA (2020), a total of 144,490 people in 14 districts of the Amhara region were affected by floods in 2019. The highest percentages of these victims were found in the two districts of the *Gumera* watershed: Fogera (27,179) and Dera (14,840). As a result, in recent climatic studies supported by GIS and Remote Sensing, understanding the variability of extreme rainfall events that will resulted to the occurrences of flood is the primary concern. However, this is only achieved based on the availability of precise and timely rainfall measurements.

Now a day, rainfall can be measured in two ways: using ground-based rain gauge stations and satellite rainfall estimates. Ground-based rain gauge stations could be used to measure the amount of rainfall observed in a specified geographical area (Alijanian et al., 2020; Reza et al., 2021). It is the most frequent and considered the most accurate device for precipitation observations (Darand and Siavashi, 2021). However, in developing countries such as Ethiopia, the availability of these stations is few and unevenly distributed (Ayehu et al., 2018; Dinku et al., 2018). Recent advances in remote sensing technology offer an alternative method for estimating rainfall amounts from satellite images (Tramblay et al., 2016; Chen et al., 2021).

There are different satellite-based rainfall products that provide nearly 40 years of rainfall time series data (Wang et al., 2017). Some of these satellites are the African Rainfall Climatology and Timeseries (TARCAT) (Dembélé and Zwart, 2016); Climate Prediction Center Merged Analysis of Precipitation CMAP) (Xie and Arkin, 1997); the Global Precipitation Climatology Project (GPCP) (Dembélé and Zwart, 2016); African Rainfall Estimate Climatology (ARC2) (Novella and Thiaw, 2013); the Tropical Application of Meteorology using Satellite and ground-based observations (TAMSAT-V3.1) (Grimes et al., 1999; Maidment et al., 2014; Tarnavsky et al., 2014); Precipitation Estimation from Remotely Sensed Information Using Artificial Neural Networks Climate Data Record (PERSIANN-CDR) and Climate Hazards Group InfraRed Precipitation with Stations (CHIRPS-V2) (Fink et al., 2021).

These satellites have their own strengths and limitations when it comes to the accuracy of rainfall estimation in various parts of the earth. The topographic complexity of the area, the instrument employed, the periods of revisit time, spatial and temporal resolution, and various algorithms are the main sources of inaccuracies observed in satellite-based rainfall products (Alijanian et al., 2019; Dinku et al., 2018; Reza et al., 2021). These factors can have an impact on the precision of satellite-based rainfall measurements, necessitating continuous performance evaluation before using the data for various applications, such as flood monitoring.

Therefore, this study aimed to evaluate the performance of satellite rainfall estimates for flood monitoring in the most flood-prone area of the Amhara Region (*Gumera* watershed), Ethiopia.

1.2. Statement of the Problem

In countries like Ethiopia, where more than 80% of the population relies on rain-fed agriculture, which is vulnerable to rainfall variability (Bewket, 2009), accurate and precise rainfall measurement is indispensable. Ethiopian National Meteorological Agency is in charge of measuring rainfall, which is done mostly by rain gauge stations located in different parts of the country. The rain gauge stations, however, are unevenly and sparsely placed throughout the country due to the complexity of the topography and other economic and technological constraints. This problem is particularly prevalent in regions like Amhara, where topographic complexity is a prominent feature.

The capacity to detect the spatial and temporal variability of precipitation is limited by the lack of rain gauge stations (Belay et al., 2019), making it difficult to monitor meteorological events like flood. As a result, in recent days, the use of satellite-based rainfall products established by various organizations at various times has grown. However, the performance of these satellite-based precipitation products must be evaluated in a regular basis before they are used in various analyses, such as flood monitoring and forecasting (Darand and Khandu, 2020). Performance evaluation of satellite rainfall estimates has recently been carried out in a number of developed countries (Fang et al., 2019; Yu et al., 2020; Darand and Khandu, 2020; Peng et al., 2021; Chiaravalloti et al., 2022).

Studies on the performance evaluation of satellite-based precipitation products across several African nations are also being conducted. (Dinku et al., 2018) conducted a study comparing satellite products with 1200 ground stations in six east African countries, including Ethiopia, Kenya, Somalia, Uganda, Rwanda, and Tanzania, and found that TAMSAT-V3.1 performed better than CHIRPS-V2 on a daily time scale, whereas CHIRPS-V2 performed better with higher skill and low or no bias than other products like ARC2. However, with unproportioned rain gauge stations, the research has a drawback in terms of vast areal coverage. Moreover, the research could not check the applicability of satellite rainfall estimates for flood monitoring in flood-prone areas.

Studies were also carried out in Ethiopia's various regions. Ayehu et al., (2018) compared the performance of satellites in the Upper Blue Nile basin and found that CHIRPS-V2 performed better than the other satellites. However, their analysis is limited to the Upper Blue Nile Basin, with 32 rain gauge stations that cover a very large area. Furthermore, they were unable to assess the satellite products' suitability for flood monitoring, as well as topographic variations, which are also not considered. Belay et al., (2019) also, evaluated the performances of CHIRPS-V2 on *Beles* Basin and shows that the performance of the satellite product can vary spatially in the study area. Despite these facts, no research on the performance evaluation of satellite rainfall estimates for flood monitoring was conducted in Ethiopia.

Therefore, the researcher is motivated to undertake this study because there is a lack of adequate literature on the performance evaluations of several satellite-based products for flood monitoring in *Gumera* Watershed, Amhara region, Ethiopia.

1.3. Objectives of the Study

1.3.1. General Objective

The general objective of the study is to evaluate the performance of satellite rainfall estimates for flood monitoring in *Gumera* Watershed of Amhara region, Ethiopia by comparing it against rain gauge station measurements.

1.3.2. Specific Objectives

The following are the specific objectives of the study:

1. To assess the trends of satellite rainfall estimates in *Gumera* watershed of Amhara region against the rain gauge measurement from 2004-2019.
2. To evaluate the accuracy of the three satellite-based rainfall products (CHIRPS-V2, TAMSAT-V3.1 and PERSIANN-CDR) against ground observations.
3. To identify the best satellite-based precipitation products used to monitor floods in *Gumera* Watershed.

1.4. RESEARCH QUESTIONS

The following are the major research questions of the study;

1. What is the trend of satellite rainfall estimates in the study area during the specified periods?
2. What is the accuracy of the three satellite-based precipitation products (CHIRPS-V2, PERSINNE CDR and TAMSAT-V3.1) in *Gumera* Watershed of Amhara Region?
3. Which satellite based precipitation product can be suitable for flood monitoring in the study area?

1.5. Significance of the Study

The finding of this study would be used for a variety of purposes in the field of geospatial and hydrological analysis. First, the study would be used to show the time series trends of rainfall from 2004 to 2019 in *Gumera* watershed. The result would be also used to determine whether or not satellite-based rainfall products can be employed in locations with few ground stations. Moreover, the study's findings could be critical in determining the suitability of satellite-based rainfall products for flood monitoring and used by the concerned offices such as disaster risk management and prevention offices. Besides, this research would serve as a model for other researchers who want to employ satellite-based rainfall data for meteorological studies and other research topics in the study area and remote sensing experts would be benefited from this study to know about the overall processes of satellite rainfall products and the way of evaluating its performances against the ground-based observation.

1.6. Scope of the Study

This study would be delimited both geographically and conceptually. The study's geographical scope is *Gumera* Watershed in Amhara National Regional State of Ethiopia, which is the most flood-prone area in the region and the study's conceptual scope is performance evaluations of satellite rainfall estimates for flood monitoring. The performances of three satellite rainfall products (CHIRPS-V2, TAMSAT-V3.1, and PERSIAN-CDR) would be evaluated against the ground-based rainfall data collected from the Ethiopian National Meteorological Agency.

1.7. LIMITATION OF THE STUDY

The following are the major limitations of the study;

- The study is limited in to *Gumera* watershed of Amhara region.
- Due to the small areal coverage, only eight stations found in and around the watershed were considered for analysis.
- Only 16 years of rainfall data downloaded from internet database were evaluated against the rain gauge measurement.
- As the result of unevenly distributed rain gauge stations point based performance evaluation approach were employed. In the future if there will be availability of adequate stations, grid to grid approaches will be employed.

1.8. Organization of the Thesis

This study is organized into five chapters. The first chapter of the study is dedicated to the introductory section; which comprises the background of the study, a brief statement of the problem, objectives, and research questions, as well as the study's significance and scope. A review of the related literatures is incorporated in the second chapter. The third chapter indicates the background of the study area as well as the research methodology employed to address the specified research questions. In the fourth chapter, the study's results and discussion are presented, and the study's summary and recommendations would be provided based on the research findings in chapter five. Finally, references used in the study and annexes would be incorporated into the last section of the thesis.

Chapter Two

2. Review of Related Literatures

2.1. Rainfall Measurement

Precipitation is one of the essential variables in meteorological and hydrological studies, and it is characterized by continuous spatial and temporal variability (Hu et al., 2019). It is also an important component of the global water cycle (Bai et al., 2018). The efficiency of various development attempts depends on accurate and precise measurement of this variable factor. These measures are also necessary to prevent calamities caused by rainfall variability, such as floods and droughts (Song et al., 2021).

In Ethiopia, the National Meteorological Agency is in charge of measuring rainfall in various areas of the country. According to the National Meteorological Agency Website, missionaries began collecting meteorological data at the end of the nineteenth century, utilizing a few stations. Ethiopian Civil Aviation Authority created a Meteorology Office in the 1950s and it was upgraded to the rank of a department in 1950s (www.ethiomet.gov.et).

A remarkable history of the department occurred in 1973 E.C when the National Meteorological Agency was established by proclamation number 201/73. These were decided in recognition of the importance of meteorology research and the exploitation of meteorological and climatic resources for economic and social development. Since its inception, the institution has taken measurements and made projections on a variety of meteorological characteristics. Measurement techniques have improved over time, and space science technology now supports them. Hence, rainfall can currently be quantified in two ways: utilizing rain gauge stations located across the country or using satellite rainfall estimates (www.ethiomet.gov.et).

2.1.1. Ground Based Rain Gauge Stations

Ground-based rain gauge stations include measurements made with a rain gauge instrument placed at a specified location. Because of its accuracy in measuring precipitation, this value is frequently used as a reference (Song et al., 2021). It was once thought to be the principal source of data for rainfall observations (Dinku et al., 2018).

According to the National Meteorological Agency website (www.ethiomet.gov.et) there are four different classes of rainfall stations. The four classes of the rainfall stations have different applications. Stations of the first class (Synoptic) are those where meteorological observations are taken for synoptic meteorology. At full GMT hours, observations are made every 24 hours a day. Stations of the second class (principal or indicative) are those that collect meteorological data for climatological reasons. Every three hours in the following GMT times, observations are taken (0300, 0600, 0900, 1200, 1500 GMT). Only three meteorological parameters are observed at third-class (Ordinary) stations: highest air temperature of the day, minimum air temperature of the day, and total rainfall amount in 24 hours and observations are made at 0600 and 1500 GMT. Stations of the fourth class (Rainfall Recording) are those that merely record the total amount of rainfall in a 24-hour period. Observations are obtained at 0600 GMT.

The quantitative resolution of gauges, on the other hand, can have an impact on accuracy. According to the National Meteorological Agency (2021), there are a total of 909 meteorological stations around the country (Meteorological stations by region: Oromia, Addis Ababa, Dire Dawa and Harari = 357, Amhara =242, Afar = 32, Somalia = 39, SNNPR (including the two recent regions) = 138, Gambela = 14, Benshangul-Gumuz = 26, Tigray = 61). These indicated that there is a proportion of a station per 1217 square kilometer areas in the country. In the Amhara region, this proportion is a single station per 701 square kilometers (NMA, 2021). These indicated that as there is a great variation of rainfall in this wide area, it is difficult to have accurate rainfall measurements in a specified area of the country which is far from the location of stations. This reality makes the use of satellite rainfall estimates indispensable in countries like Ethiopia and regions such as Amhara where there is a highly dispersed distribution of ground-based rain gauge rainfall stations.

2.1.2. Satellite Rainfall Estimates

Rainfall can also be measured from satellite products. Satellite-based rainfall estimations can offer data in places where there are no rainfall stations or aid to improve data in areas where there is a sparse density of stations. The global coverage of space-based precipitation estimates is a major benefit, as it provides information on rainfall frequency and severity in areas where other monitoring methods such as rain gauges and radar are not installed. The drawback is that they are only estimations of rainfall, as they are dependent on cloud top features (in the case of IR algorithms) as well as cloud liquid and ice content (in the case of passive microwave algorithms). This study describes the three high-resolution satellite-based rainfall data sets used in this investigation.

Though there are different types of satellites that are used for precipitation measurements, Climate Hazards Group InfraRed Precipitation with Station data (CHIRPS-V2), Precipitation Estimation from Remotely Sensed Information Using Artificial Neural Networks Climate Data Record (PERSIANN-CDR) and Tropical Application of Meteorology Using Satellite (TAMSAT-V3.1) are selected for this study. The selection was made based on three criteria including spatial resolution, provision of long time series data, and freely and easily availability. The major features of the three satellites are explained as follows.

Climate Hazards Group Infra-Red Precipitation with Station data (CHIRPS-V2)

Climate Hazards Group Infra-Red Precipitation with Station data (CHIRPS-V2) is developed by the US Geological Survey and the Climate Hazards Group at the University of California at Santa Barbara (https://www.chc.ucsb.edu/data). The Climate Hazards Group's Infrared Precipitation with Stations (CHIRPS-V2) dataset builds on past efforts to use smart interpolation techniques and high-resolution, long-term precipitation estimates based on infrared Cold Cloud Duration (CCD) observation. The algorithm of this satellite has the following major features (Funk et al., 2015): (1) It is based on a 0.05° climatology that uses satellite data to represent sparsely gauged locations; (2) Includes daily, pentadal, and monthly 0.05° CCD-based precipitation estimates from 1981 to the present; (3) Blends station data to produce a preliminary information product with a latency of about 2 days and a final product with an average latency of about 3 weeks; and (4) Uses a novel blending. CHIRPS-V2 can be used to quantify the hydrologic impacts of decreasing precipitation and rising air temperatures in the Greater Horn of Africa by presenting the CHIRPS-V2 algorithm, global and regional validation results (https://www.chc.ucsb.edu/data).

Tropical Application of Meteorology Using Satellite (TAMSAT-V3.1)

TAMSAT-V3.1 is a satellite built by the University of Reading's research division, and it delivers rainfall predictions across Africa based on TIR images taken every 15 minutes (30 minutes before to June 2006) and ground-based measurements. The TAMSAT-V3.1 method is based on linear correlations between rain gauge records and the number of hours when TIR pixel brightness temperatures fall below a specific rain/no-rain temperature threshold known as the cold cloud duration (CCD) (Bai et al.,2018).

This is a satellite that helps African meteorological authorities and other organizations by delivering and promoting satellite-based rainfall estimates and related data products. TAMSAT-V3.1 delivers daily rainfall estimates with a 4km resolution for all of Africa. The TAMSAT-V3.1 archive covers the years 1983 through the present. The dataset's lifetime makes it particularly well suited to risk assessment. The data can be used for famine early warning, drought insurance, and agricultural decision assistance, among other things (Maidment et al., 2017).

Rainfall estimates and other TAMSAT-V3.1 product are released on the first, sixth, eleventh, sixteenth, twenty-first, and twenty-sixth days of each month. TAMSAT-V3.1 data is available under a creative commons license for operational, research, and commercial usage.

TAMSAT-V3.1 was founded in 1977 at the University of Reading. To expand the breadth of climate services it provides, the group has formed tight cooperation with the

Climate Division of the National Centre for Atmospheric Science (NCAS) and the National Centre for Earth Observation (NCEO) over the previous three years. These partnerships are assisting in the creation of new datasets and other products, such as rainfall estimate uncertainty, whole column soil moisture, and probabilistic drought forecasts (http://www.TAMSAT-V3.1.org.uk/data/).

Precipitation Estimation from Remotely Sensed Information Using Artificial Neural Networks Climate Data Record (PERSIANN-CDR)

PERSIANN-CDR is developed by the Center for Hydrometeorology and Remote Sensing (CHRS) at the University of California. It estimates daily rainfall at 0.25 degree for spatial coverage of 60^0N to 60^0S from January 1, 1983, to the present. The goal of PERSIANN-CDR is to address the need for consistent, long-term, high-resolution global precipitation datasets that can be used to study daily precipitation variability and trends. The PERSIANN-CDR dataset is derived from the PERSIANN algorism using GridSAT-B1 infrared data and adjusted using the Global Precipitation Climatology Project (GPCP) monthly product to ensure consistency of the two datasets at similar spatial resolution throughout the entire record. The product is free to the public as an operational climate data record on the NOAA NCDC CDR Program website under the atmospheric CDRs Category (https://chrsdata.eng.uci.edu/).

2.2. Evaluation of Satellite Rainfall Estimate for Flood Monitoring

Despite the fact that various research has been undertaken on the performance evaluations of satellite-based data, the majority of them have been unable to demonstrate its usefulness for meteorological analysis including flood and drought monitoring. Peng et al., (2021) assess the performance of satellite-based products in Central Asia, finding that: 1) The GPM and CDR datasets were the best for daily and monthly scale rainfall accuracy ratings, respectively. 2) At different locations in a watershed, the performance of CDR and GPM was more consistent than that of other datasets, and all datasets tended to perform better in humid regions. 3) In comparison to other datasets, all datasets performed better in the summer of a year, but the CDR and CHIRPS-V2 fared well in the winter. 4) In monthly runoff simulations, CDR and CMORPH raw data fared better than others, notably CDR. 5) by combining the hydrological performance of uncorrected and corrected data, all datasets can give useful input data for hydrological modeling.

Yu et al., (2020) also assesses the performance of three satellite-based products from 2015 to 2018, including CHIRPS-V2, GPM-IMERG, and PERSIANN-CCS. Despite the short temporal coverage, the results demonstrate that satellite-based products perform well in the summer and have a high bias in the spring. It performs poorly in the cold, with a low chance of detection and a high proportion of false alarms. The performance of satellite-based data in terms of precipitation spatial expression varies among basins. From the southeast shore to the northwest hinterland, the gradient features are visible. The products can represent extreme precipitation occurrences to some extent, although their performance is significantly inferior to that of a rain gauge. The study prevailed that, among the three satellites, GPM-IMERG shows best expression of precipitation.

The CHIRPS-V2, TAMSAT-V3, and ARC 2 satellites' performance in Eastern Africa was also assessed on a daily, decadal, and monthly time scale (Dinku et al., 2018). The results showed that CHIRPS-V2 products outperform ARC2 in terms of skill and bias, with a lower or no prejudice. At dekadal and monthly time periods, these products were determined to be marginally better than TAMSAT-V3 product, whereas TAMSAT-V3 performed better at the daily time scale. The performance of the various satellite products varies greatly across space, with particularly poor results in coastal and hilly areas. As a result, in places with complicated topography like the Amhara region, the performance of such satellites must be reviewed over time.

In addition to performance evaluation of satellite rainfall estimates, some researches were also conducted on the application of these data for flood monitoring. Tote et al., (2015) conducted a study to evaluate satellite rainfall estimates performance for flood and drought monitoring in Mozambique. The satellites include TAMSAT, African Rainfall Climatology and Time-series (TARCAT) v2.0, Famine Early Warning System NETwork (FEWS NET) Rainfall Estimate (RFE) v2.0, and Climate Hazards Group InfraRed Precipitation with Stations (CHIRPS-V2)) and the study's findings revealed that the RFE and CHIRPS-V2 products perform as well as TARCAT on the majority of statistical measures of skill. TARCAT detects the relative frequency of rainfall events the best, while RFE underestimates and CHIRPS-V2 overestimates the frequency of rainfall events.

Setiawati & Miura (2016) also assessed the performance of GSMaP Daily Rainfall Satellite Data for Flood Monitoring in Japan, concluding that GSMaP may significantly underestimate heavy rainfall. However, it is not possible to find researched conducted in Ethiopia that aim to evaluate the performances of satellite rainfall estimates for flood monitoring.

2.3. Flood in Amhara Region

Flooding has had a significant impact on Ethiopian communities and economies. It is becoming more common in the country, causing significant loss of life and property. The following table from Alemu and Assaye (2020) shows the number of affected households in the area of *Gumera* watershed due to the flood occurred in 2019.

Table 1: Number of affected households by the 2019 flood in *Gumera* Watershed

Districts	Number of Affected Households			Number/Name of Affected Sub-districts
	M	F	Total	
Fogera	6614	756	7370	Shaga, Shina, Kidist Hana, Ava Kokit, Nabega, Wagetera, Kuhar Michael, and Tiwaza Kena
Dera	2705	349	3054	Jigena, Zara, and Tana Dinbiso
Total	9319	1105	10424	More than 11 sub-districts

Source: (Alemu and Assaye, 2020)

Chapter Three

3. Material and Methodology

3.1. Description of the Study Area

3.1.1. Location of *Gumera* Watershed

Gumera watershed, drained by *Gumera* River is located in Amhara national regional state of Ethiopia, at 624 Km Northwest of Addis Ababa. Astronomically, the watershed is located within 11°35'00''N and 11°58'00''N and 37°50'00''E and 38°11'00''E. This watershed is part of the *Abay* Basin, particularly the Lake *Tana* sub-basin, which is located on the Northeastern side of Lake *Tana*. The watershed drained four districts of *Amhara* national regional state including the *Dera*, *Farta*, *Fogera*, and *Estie* districts. The following figure shows the location and elevation of *Gumera* Watershed.

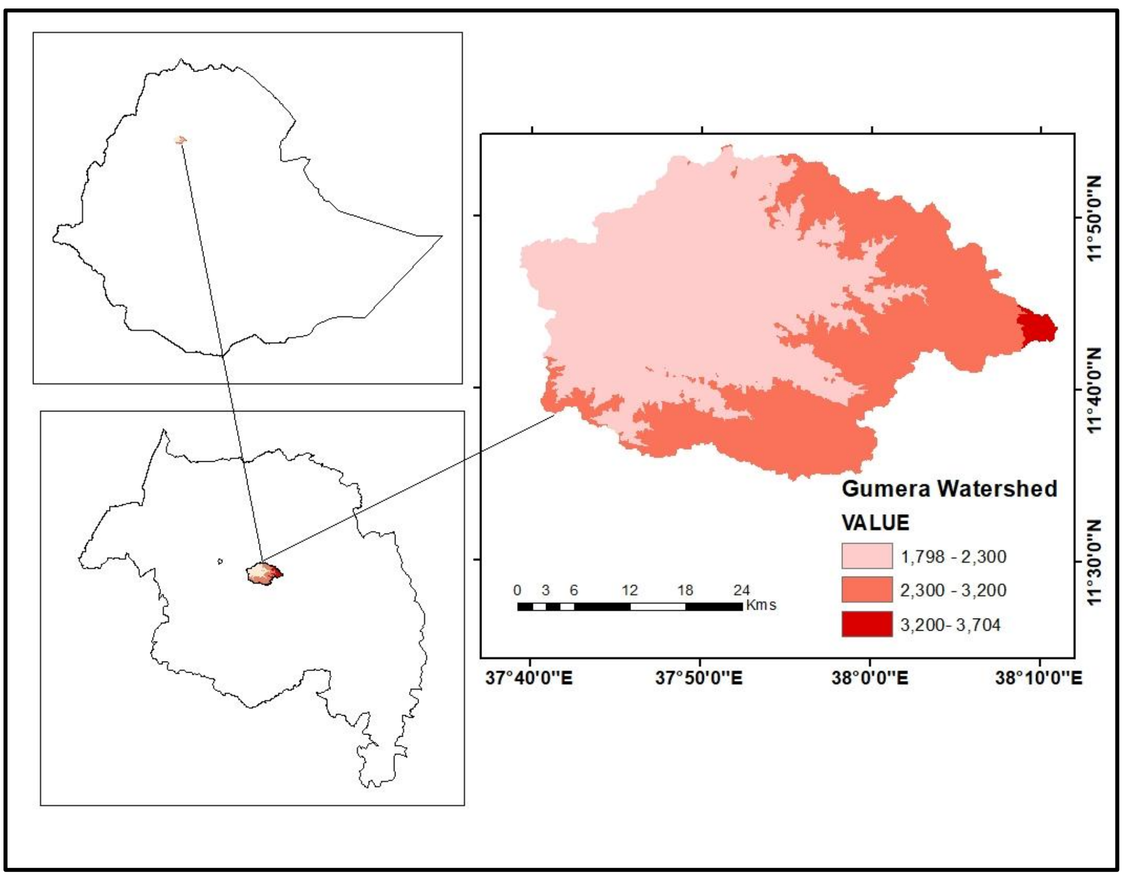

Figure 1: Location map of the study area

As shown in the above figure, Gumera watershed is found in three agroclimatic zones; Weyna Dega, Dega and Wurch. Relatively, Weyna dega and dega agroclimatic zones covers the largest proportion.

3.1.2. Watershed Delineation

The process of identifying the drainage area of a point or set of points is known as watershed delineation (Tian, 2017). As an input, an elevation raster or Digital Elevation Model (DEM) can be used to automatically delineate and quantify the characteristics of a drainage system. DEMs store the same information that contour lines do, but in a different structure.

The study area watershed has been developed from the Digital Elevation Model (DEM) of Ethiopia. The watershed delineation was conducted by using different preprocessing activities in ArcGIS 10.8. The major processes include fill, flow direction, flow accumulation, and creating outlet (pour) points. The hydrological gauge station located on the river at located at 11°50’0” N latitude and 37°38’ 0” E longitude is used as a pour point. After the outlet (pour) point was created, the watershed delineation was made. The final watershed delineation map is used to prepare the location map of the study area indicated in Figure 1.

3.1.2. Climate and Hydrology

In Ethiopia, there are three distinct rainfall seasons including *Kiremt* (June-September), Bega (October-January) and *Belg* (February-May). From these seasons *Kiremt* is the primary rainy season and *Bega* is the dry season, whereas *Belg* is the small rainy season. The *Gumera* watershed has a relatively temperate climate due to its high elevation (3704 m). Based on data from 1961 to 2000 (Gamachu, 1977; Setegn, et al., 2009a), the projected mean annual precipitation ranges from 1200 to 1600 mm, with more than 80 percent of yearly rainfall falling between May and September. Although there is a diurnal temperature fluctuation, the temperature at Bahir Dar is quite consistent throughout the year, with an average yearly temperature of 20.2°C. From 1994 to 2004, the average daily maximum and minimum temperatures in Bahir Dar were 27.2°C and 13.2°C, respectively.

3.2. Research Methodology

3.2.1 Data Sources

Ethiopian National Meteorological Agency, Fogera district agricultural office and internet database are the major data sources of this study. Rainfall data from ground-based meteorological stations were collected from the Ethiopian National Meteorological Agency, while historical flood events data were collected from the *Fogera* district agricultural office. The Remote sensing satellite rainfall estimates of the three satellite rainfall products were collected from different digital databases. Additionally, DEM data would be used to investigate the characteristics of satellite rainfall estimates of the study area in relation to different aspects. The following section discusses the applicability of these data in achieving the study's objectives.

Ground Based Rainfall Data

Rainfall data of the stations from 2004 - 2019 were collected from the Ethiopian National Meteorological Agency (NMA). As it is recommended by different researchers, 15 years or above data are appropriate to evaluate the performances of satellite rainfall estimates for flood monitoring. Besides, the upper limit of the study period was decided based on the availability of the data at NMA. Considering these, 16 years of rainfall data were considered by this study. The ground-based rainfall data has been collected from all class stations found in and near to the study watershed. Eight stations found in and near to the watershed were primarily considered for this study. These include *Wenzaye*, *Debre Tabor*, *Wereta, Hamusit, Ambesame, Agere Genet, Bahir Dar Airport* and *Bahir Dar new*. The latitudinal and longitudinal locations and elevations of the eight meteorological stations are indicated on table 2.

Table 2: Locations and Elevations of Stations found in and nearby the *Gumera* Watershed

Stations	**Location**		**Elevation**
	X	Y	
Wenzaye	11.7862	37.67503	1821
Debre Tabor	11.8666	37.9954	2612
Wereta	11.92225	37.6958	1819
Dera Hamusit	11.77	37.38	1900
Ambesame	11.69982	37.62485	2076
Agere Genet	11.8005	38.2987	3010
Bahir Dar A. P	11.6027	37.322	1827
Bahir Dar New	11.595	37.36	1800

Source: National Meteorological Agency, 2022

Table 3 shows the mean, standard deviation, and percentage of missing data of the annual rainfall from 2004 to 2019 observed at the eight meteorological stations. The highest mean annual rainfall during the specified period was observed at *Agere genet* station, followed by the two meteorological stations located in *Bahir Dar*. Because of the highest percentage of missing data (54.68 and 34.4 percent), *Dera Hamussit* and *Ambessame* stations were not included in the analysis.

Table 3: Mean and Standard Deviation of annual rainfall from 2004 -2019

Stations	Annual Rainfall		% of Missing Data
	Mean	Std.	
Wenzaye	1435.13	189.57	1.56
Debre Tabor	1515.78	202.82	0.00
Woreta	1372.35	336.3	6.25
Dera Hamusit			54.68
Ambesame			34.4
Agere Genet	1688.31	343.09	1.56
Bahir Dar Airport	1554.34	243.42	0.00
Bahir Dar New	1554.34	243.42	0.00

Source: National Meteorological Agency, 2022

The completeness and consistency of the data collected from these stations were checked to compare with the satellite rainfall estimations.

Satellite based Rainfall products

For this study, three satellites (Tropical Applications of Meteorology using Satellite and ground-based observations, Precipitation Estimation from Remotely Sensed Information Using Artificial Neural Networks Climate Data Record, and Climate Hazards Group InfraRed Precipitation with Stations) were selected based on three primary criteria's: high spatial resolution, lengthy time series data, and free availability and easily accessibility of the data. The general characteristics of the three satellites are indicated below in Table 4.

Table 4: Characteristics of CHIRPS-V2, TAMSAT-V3.1 and PERSIANN-CDR

No.	Satellite Rainfall Products	Period	Spatial Resolution	Temporal resolution	Coverage	Reference
1	CHIRPS-V2	1981-present	0.05^0	Daily	50^0N-50^0S	https://www.chc.ucsb.edu/data
2	TAMSAT-V3.1	1983-present	0.0375	Daily, Pentadal, Dekadal	Africa	http://www.TAMSAT-V3.1.org.uk/data/
3	PERSIANN-CDR	1983-present	0.25^0	Daily	60^0N-60^0S	https://chrsdata.eng.uci.edu/

As the primary aim of the study is to evaluate the performance of the three satellite rainfall products for flood monitoring, the *kiremt* season including the months of June, July, August, and September rainfall was considered. Thus, for the stated research period, 16-year annual, 64 monthly, and 1952 daily rainfall data were compared with the ground station measurements. Moreover, the performances of the satellite rainfall products were also evaluated against the rainfall measurements during the flood events that occurred in the study area during the specified study period.

History of Flood Events in the *Gumera* Watershed

Flood occurs in different areas of the region in different times. This study focused on the occurrences of flood in the region between 2004 and 2019. The time when flood occurs were checked with the satellite rainfall estimates and the better satellite that detects the occurrences of floods was identified. Hence, historical data that shows the occurrences of flood in the stated periods would be collected from *Fogera* district Agriculture office.

3.2.2. Sampling procedures and Design

As the main aim of the study is to evaluate the performances of satellite rainfall estimates for flood monitoring, the study area is selected purposively. The main criteria used to select the study area were occurrences of flood and topographic complexity. Hence, Amhara regional State was selected based on the complexity of topography and the most flood-prone area (*Gumera* Watershed) was selected to check the applicability of satellite rainfall estimate for flood monitoring.

3.2.3. Data Collection Procedures

The data were collected in two consecutive phases. In the first phase, 16 years (2004-2019) rainfall data that were collected by rain gauge stations and historical flood events in *Gumera* watershed were collected from Ethiopian National Meteorological Agency (NMA) and District agricultural office respectively. The rainfall data were collected on a daily basis and then processed into different timescales based on necessity.

In the second phase, satellite rainfall estimates were downloaded from three freely available satellites; CHIRPS-V2 from https://www.chc.ucsb.edu/data; PERSIANN-CDR from https://chrsdata.eng.uci.edu/ and TAMSAT-V3.1 from http://www.TAMSAT-V3.1.org.uk/data/. These data were passed through image processing based on the needs of the data and compatibility with the rain gauge point data.

3.2.4. Methods of Data analysis and interpretation

The data collected from both rain gauge measurements and satellite-based products were employed for the analysis. Both remote sensing techniques and statistical indices were used to evaluate the performances of satellite rainfall estimates for flood monitoring.

Evaluation of Satellite based products

To evaluate the performance of satellite rainfall estimates with rain gauge observations, there are two types of approaches: point to grid (point-based) and grid to grid (interpolated grid to satellite grid) (Duan et al., 2016).

Grid-to-grid evaluation is performed after point-based rainfall measurements are interpolated using several interpolation techniques. This method of evaluation is appropriate when the area is covered by a large number of gauge stations that are all connected in a uniform manner (Ayehu et al., 2018).

The point-to-grid approach is computed by using the point data collected by rain gauge and grid satellite rainfall estimates. This type of methodology is critical for evaluating satellite-based products in places where rain gauge stations are scarce, unavailable, or unevenly distributed (Dinku et al., 2018). As a result of the sparse and uneven distribution of rain gauge stations in the study area, the point to grid (point-based) evaluation method was employed. For this purpose, the satellite data were downloaded in

NetCDF format and the data were generated from the file using the locations of ground rain gauge stations and organized in Microsoft Excel.

After the data were organized in a proper manner, two types of statistics have been employed to evaluate the performances of satellite rainfall estimates against the measured rainfall data: these include continuous statistics which would be used to evaluate the performance of satellite products in estimating the amount of rainfall and categorical validation statistics that evaluate rain detection capabilities of satellites. The indices employed by the study are explained as follows;

Continuous Statistical Indices: the performances of the three satellite estimates were evaluated using the following four continuous statistical indices in terms of annual, seasonal, monthly and daily temporal scales.

Pearson correlation coefficient (r): the Pearson correlation coefficient is a continuous statistical index that measures the linear relationship between the satellite rainfall estimates with observed rain gauge data. The value of the Pearson correlation coefficient lies between negative one and positive one. A positive value indicates a positive linear relationship while a negative value reflects an inverse linear relationship between the estimated and observed rainfall data. One is the perfect score of the Pearson correlation coefficient which shows there is a perfect linear relationship.

Mean error (ME) and Root mean Absolute error (RMAE): The Mean error and root mean absolute error helps to identify the average error occurred in the estimation data from the observed rainfall data. The value of these indices ranges from minus infinity to plus infinity and zero is the perfect score.

*Bia*s: Bias is the other continuous statistical index helps to check the relative bias of rain gauge data from satellite-based products. The perfect score of Bias is one.

Nash-Shtcliffe Efficiency Coefficient (Eff): Nash-Shtcliffe Efficiency Coefficient is an index that shows the skill of the estimates in relation to the gauge mean. The result of "Eff" varies from minus infinity to one and the gauge mean is a better estimate with negative values, zero indicates the gauge mean is as good as the estimate and one corresponds to a perfect match between the gauge data and satellite-based data. Table 1 showed the continuous verification statistics, formulas and perfect score.

Table 5: Continuous Statistical Indices

Statistics	Formula	Perfect Score
Pearson correlation coefficient (r)	$\frac{\sum(G-\vec{G})\,(S-\vec{S})}{\sqrt{\sum(G-\vec{G})^2)}\sqrt{\sum(S-\vec{S})^2)}}$	1
Mean Error (ME)	$1/N\sum(S-G)$	0
Root mean absolute error (RMAE)	$1/N\sum\lvert(S-G)\rvert)/(\vec{G})$	0
Nash-Sutcliffe Efficiency coefficient (*Eff*)	$1-(\sum(S-G)^2/\sum(G-\vec{G})^2)$	1
Bias	$\frac{\sum S}{\sum G}$	1

Where: G stands for gauge rainfall observations, S stands for satellite rainfall estimates, $\vec{G}$ stands for average gauge rainfall observations, $\vec{S}$ stands for average satellite rainfall estimates, and n stands for the number of data pairs.

Categorical validation Statistics: these statistical indices were used to evaluate the performances of satellite rainfall estimates to detect the actual observed rainfall amount.

The most commonly used categorical statistics include; Probability of detection (*POD)*, False alarm ratio (*FAR*) and Critical success index (*CSI*).

Probability of Detection (*PoD*): this statistical measure indicates what fraction of the observed events was correctly estimated.

False Alarm Ratio (*FAR*): it indicates what fraction of the estimated events did not actually occur.

Critical Success Index (*CSI*): is a statistical parameter which serves to assess the rain-detection capability of satellite rainfall estimates in relative to the ground gauged data records. The result of CSI rages from Zero to One and one is the perfect score whereas, zero indicates less detection capabilities. The following table shows the three categorical validation statistics with its formulas and perfect score.

Table 6: Categorical validation statistics

Statistics	Formula	Perfect Score
Probability of detection (*PoD*)	H/(H+M)	1
False alarm ratio (*FAR*)	F/(H+F)	0
Critical Success Index (*CSI*)	H/H+M+F	1

Where: H = number of hits, M = number of misses, and F = number of false alarms

To verify the frequency of the correct and incorrect estimated values, four combinations between the estimated and observed data can be done. These combinations are suggested by Ebert (2007) in a contingency table indicated as follows:

Table 7: Contingency table

Gauge Rainfall	Satellite rainfall	
	No rain	Yes rain
No rain	Correct Negative (N)	False Alarm (F)
Yes Rain	Miss (M)	Hit (H)

The probability of detection (PoD) is the likelihood of observed rainfall days being accurately estimated by satellite rainfall products. It displays the percentage of satellite rainfall products that successfully detected the presence of rainfall events. The false alarm ratio computes the proportion of occurrences identified by satellite rainfall products but not confirmed by observed data. The critical success index, also known as the equitable threat score, assesses the satellite's overall ability in relation to rain gauge observations by combining the aspects of hits, misses, and false alarms. These indices are critical for comparing the three satellite rainfall datasets for flood monitoring. The categorical statistical indices (PoD, FAR and CSI) were conducted for the daily, monthly and seasonal rainfall estimates of the study period.

Moreover, the performance of satellite rainfall estimates would be also evaluated using rainfall categories. The rainfall categories would help to investigate the satellite capability of recording lowest as well as highest amount of rainfall observed by the gauge stations. Satellite rainfall dataset that has a good capacity of estimating the highest category of rainfall will have the best satellite dataset that will help to monitor floods. This would be evaluated using the daily observed rainfall of the study period and flood occurrence periods.

The overall work flow of the study would be indicated on Figure 4. The work flow indicates three major input data; satellite rainfall products, ground-based rainfall data, and historical flood events. The satellite rainfall products include CHIRPS-V2, TAMSAT-V3.1, and PERSIANN-CDR. The estimations from these datasets were evaluated by the ground-based rainfall observations using both continuous and categorical statistics. Moreover, a graphical comparison was also conducted to show the variation of rainfall estimates with the observed data.

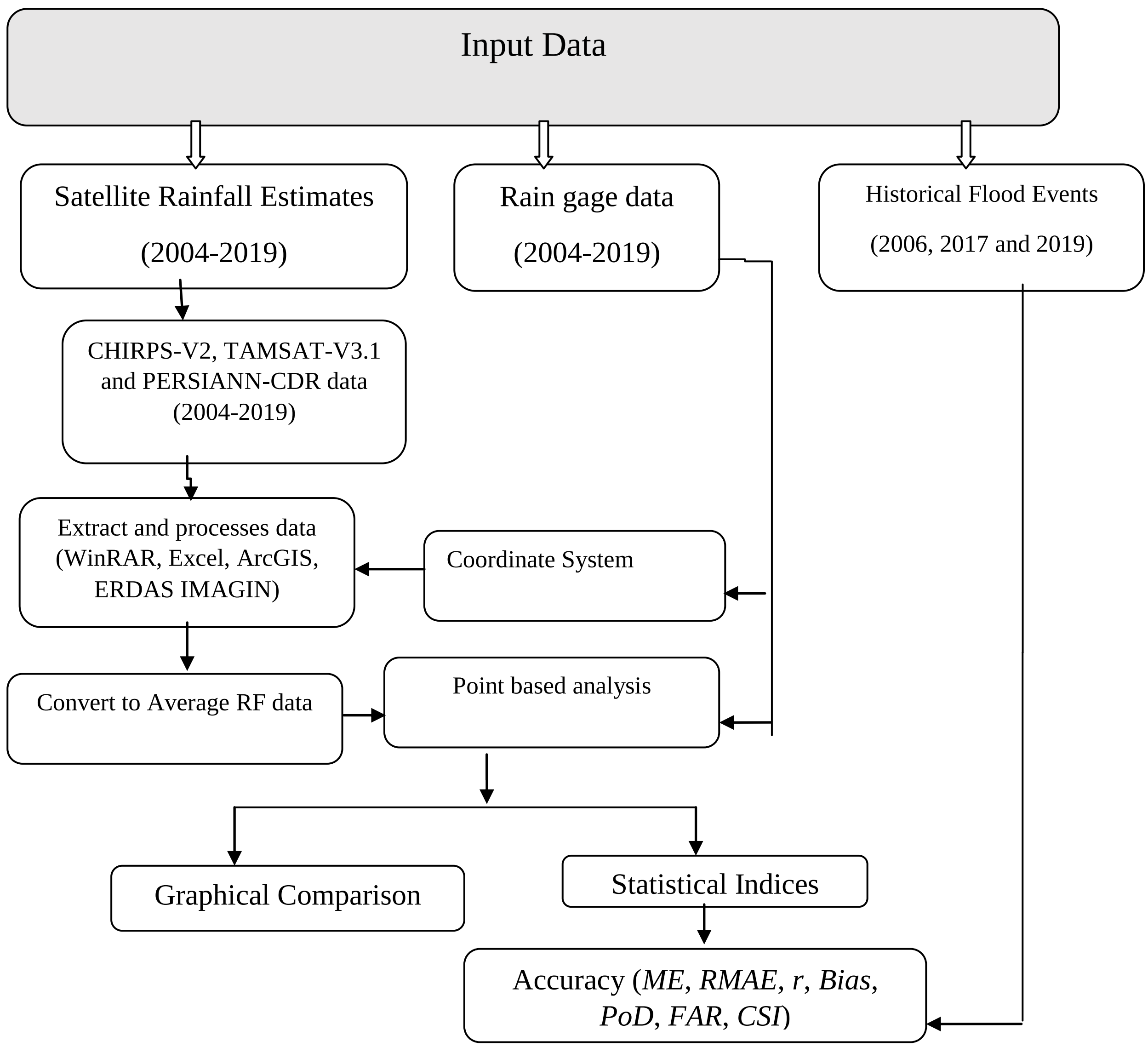

Figure 2: Schematic diagram of the research framework

Chapter Four

4. Result and Discussion

4.1. General Trends of Rainfall Estimates in the *Gumera* Watershed

The first main task of this study is to check the general trend of observed and estimated rainfall in the study area. The mean annual rainfall recorded by the ground rain gauge stations and estimated by the three satellite rainfall products is indicated on Table 8. According to the ground station measurement, the highest mean annual rainfall was recorded in 2008 with 1721.42 mm, followed by the mean annual amount of precipitation recorded in 2010 and 2006 with 1703.74 mm and 1683.32 mm, respectively, whereas, the lowest mean annual rainfall was recorded in 2004 with 1143 mm, followed by the rainfall recorded in 2005 with 1441.48 mm.

Table 8: Annual Average rainfall (mm) of *Gumera* Watershed from 2004-2019

Year	Gauge	CHIRPS-V2	TAMSAT-V3.1	PERSIANN-CDR
2004	1143	1158.64	1072.16	1298.55
2005	1441.48	1302.68	1351.68	1049.29
2006	1683.32	1589.79	1391.9	1391.87
2007	1565.74	1393.96	1384.92	1126.46
2008	1721.42	1488.75	1465.96	1343.67
2009	1250.96	1084.51	1122.84	880.84
2010	1703.74	1417.45	1680.34	1102.29
2011	1552.78	1419.66	1368.08	1088.58
2012	1507.92	1458.13	1409.34	1084.79
2013	1646.28	1500.42	1442.86	1069.74

2014	1545.14	1462.49	1443.88	1298.55
2015	1532.4	1233.44	1357.68	1151.75
2016	1513.45	1456.79	1381.05	1080.96
2017	1323.08	1565.08	1505.62	1252.59
2018	1544.48	1435.93	1307.5	1222.54
2019	1563.88	1652.52	1464.62	1301.14

Source: NMA (2022), https://www.chc.ucsb.edu/data, http://www.TAMSAT-V3.1.org.uk/data/ and https://chrsdata.eng.uci.edu/

As depicted in table 8 above, the three satellite datasets also estimated the mean annual rainfall. According to the CHIRPS-V2 dataset, the highest mean annual rainfall was estimated in 2019, followed by 2006 with 1652.52 mm and 1589.79 mm respectively, whereas TAMSAT-V3.1 and PERSIANN-CDR recorded the highest amount of mean annual rainfall in 2010 and 2006 with 1680.34 mm and 1391.87 mm respectively. These indicates TAMSAT- V3.1 recorded highest amount of rainfall (1680.34 mm) than CHIRPS V-2 and PERSIANN-CDR during the study period.

Figure 3 also shows the distribution of observed and estimated mean annual rainfall from 2004 to 2019. As the graph shows, CHIRPS-V2 estimated the highest mean annual rainfall over the gauge observations in 2004, 2017, and 2019, while TAMSAT-V3.1 and PERSIANN-CDR had the highest mean annual rainfall estimation over the rain gauge observations only in 2017 and 2014, respectively.

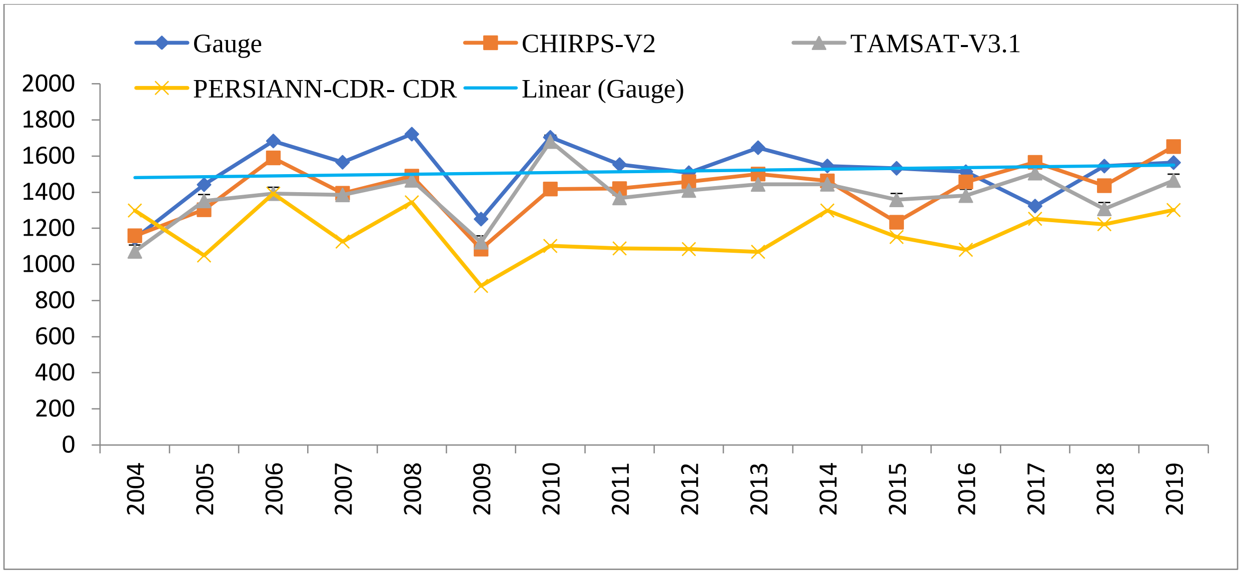

Figure 3: Average Annual rainfall distribution of Gauge, CHIRPS-V2, TAMSAT-V3.1 and PERSIANN-CDR

Source: NMA (2022), https://www.chc.ucsb.edu/data, http://www.TAMSAT-V3.1.org.uk/data/ and https://chrsdata.eng.uci.edu/

Figure 3 also indicate the linear trendlines of the observed rainfall in the study area, which indicates lowest variation of annual rainfall in the study areas during the study period. Karam et.al, (2020) also identified that there is no statistically significance rainfall trend in Ethiopia from 1961 to 2015.

Figure 3 also shows the highest and lowest variation between the estimated and observed amounts of the mean annual rainfall from 2004 to 2019. CHIRPS-V2 estimation had the lowest and highest variation from the observed gauge station in 2004 and 2015, with values of 15.64 mm and 298.96 mm, respectively. TAMSAT-V3.1 estimation had the lowest and highest variation from the observed gauge station in 2010 and 2006, with values of 23.4 mm and 291.42 mm, respectively, and PERSIANN-CDR estimation had the lowest and highest variation in 2017 and 2010, with values of 70.49 mm and 601.45 mm. This indicates, in the lowest and highest mean annual rainfall of the *Gumera* watershed CHIRPS-V2 and TAMSAT-V3.1 had better agreement with the observed rainfall respectively.

To evaluate the performance of satellite rainfall estimates for flood monitoring, considering the rainfall of the *kiremt* season is vital. As stated by Setegn et al., (2009), Ethiopia as a country has three major rainfall seasons, including the *Kiremt*, *Belg*, and *Bega* rainfall seasons. However, the occurrence of floods is observed during the *Kiremt* rainfall season, which mainly includes four months of the year; June, July, August, and September. Therefore, this study aimed to check the trends of observed and estimated rainfall during the four months of the *Kirmet* season. Figure 8 indicates the mean rainfall of *the kiremt* season in the *Gumera* watershed from 2004 to 2019.

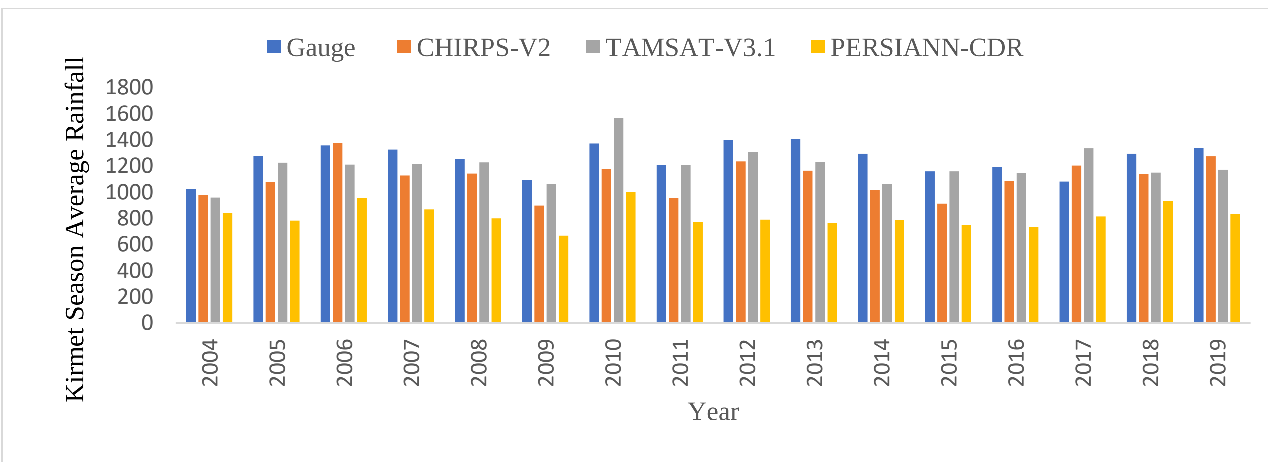

Figure 4: Trends of Mean rainfall of *Kiremt* Season (June-September) in *Gumera* watershed from 2004 to 2019

Source: NMA (2022), https://www.chc.ucsb.edu/data, http://www.TAMSAT-V3.1.org.uk/data/ and https://chrsdata.eng.uci.edu/

As indicated in Figure 4, TAMSAT-V3.1 had the highest estimation over the observed gauge rainfall measurements in 2010, and 2017. CHIRPS-V2 estimated the mean seasonal rainfall of the area as higher than the observed gauge measurements in 2006 and

2017. From the three satellite datasets, PERSIANN-CDR had lower mean seasonal rainfall estimations than the observed gauge stations throughout the research period.

Figure 5 shows the monthly distribution of the estimated and observed rainfall of *Gumera* watershed from 2014 to 2019. CHIRPS-V2 and TAMSAT-V3.1 estimated the mean monthly rainfall of the area better than the estimation of PERSIANN-CDR, which had the lowest estimation throughout the research period.

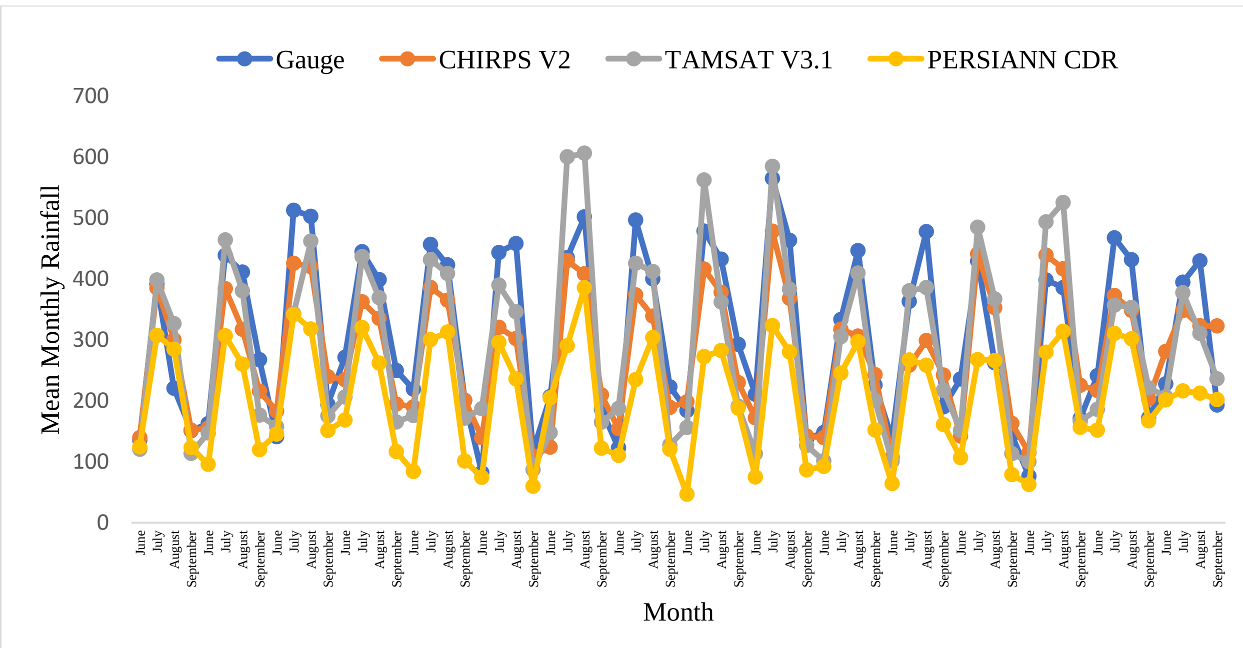

Figure 5: Monthly Trends of rainfall in *Gumera* watershed from 2004 to 2019

Source: NMA (2022), https://www.chc.ucsb.edu/data, http://www.TAMSAT-V3.1.org.uk/data/ and https://chrsdata.eng.uci.edu/

Moreover, the rainfall trends of the *Gumera* watershed were observed from the six stations and the satellite estimates. There were variations in the observed rainfall in every month of the study period. Ayalew et al. (2012) also identified the monthly variable trends of rainfall in the Amhara region of Ethiopia.

The long-term mean annual rainfall of the watershed is 1518.4 mm. However, there is spatial variation in the long-term mean annual rainfall. From the six rain gauge stations, the highest and lowest long-term mean annual rainfall were recorded in *Woreta* and *Agere Genet* stations with 1372 mm and 1688 mm, with a standard deviation of 336.3 and 343.09 respectively. This variation is directly correlated with the elevation of the area (elevation of *Woreta*, 1819 and Agere genet, 3010), which proves the fact that rainfall increases with increasing elevation.

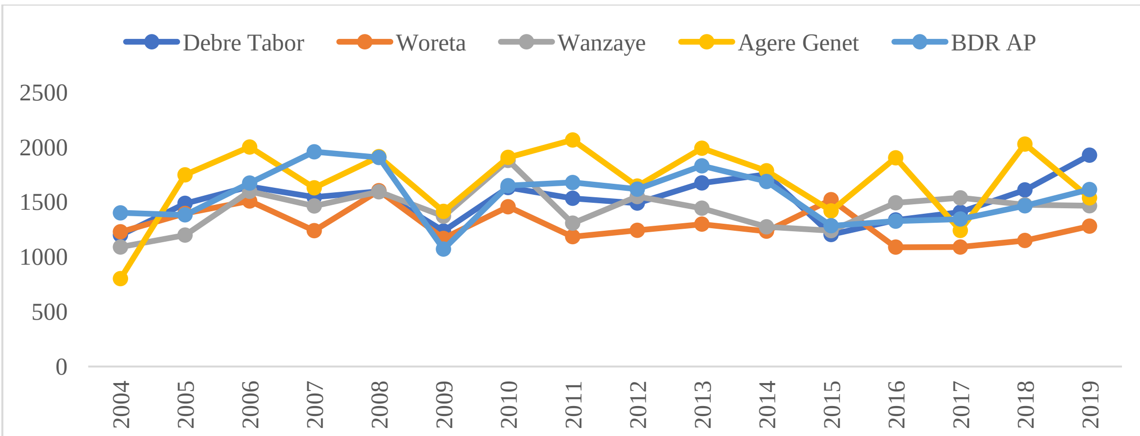

Figure 6: Trends of Mean annual rainfall in the separate stations.

The *kiremt* season's long-term mean seasonal rainfall of the watershed is 1234 mm. However, the spatial variation of rainfall is still observed on a seasonal basis. From the six stations, the highest *kiremt* season long-term rainfall was observed at Bahir Dar stations with 1329mm, followed by *Agere Genet* station with 1314mm, and the lowest *kiremt* season long-term mean rainfall was observed at *Woreta* station with 1156 mm, followed by Debre Tabor station with 1167 mm.

4.2. Evaluation of Satellite Rainfall

The satellite estimates were evaluated using continuous statistics (r, ME, RMAE, and Bias) at annual, seasonal, monthly, and daily temporal scales and categorical statistical indices (PoD, FAR, and` CSI) on a daily temporal scale.

4.2.1. Annual Rainfall Evaluation

The mean annual rainfall data of the three satellite rainfall estimates were compared with the rain gauge station measurements. Continuous statistical indices, including the correlation coefficient (r), mean error (ME), root mean absolute error (RMAE), Bias (Bias), and Nash-Sutcliffe efficiency coefficient (E*ff*), were employed for the performance evaluation of satellite rainfall estimates in the *Gumera* watershed from 2014 to 2019.

As stated by different scholars (Ayehu et al., 2018; Dinku et al., 2018; Shari et al., 2018); in annual rainfall evaluation, rain detection capabilities through categorical statistical indices are not a concern. Therefore, the evaluation of annual rainfall estimation was conducted only using continuous statistical indices.

As indicated in Table 10, in terms of annual temporal scale, TAMSAT-V3.1 rainfall estimation had better agreement with the rain gauge measurements than CHIRPS-V2 and PERSIANN-CDR, with the highest correlation coefficient, the lowest ME, and RMAE. TAMSAT-V3.1 had a correlation coefficient (r) value of 0.74, and ME and RMAE of -19.68 and -0.013, respectively. The CHIRPS-V2 dataset had the second-best agreement, with a correlation coefficient of 0.62. Whereas, PERSIANN-CDR had the poorest agreement with the observed data, with the least correlation coefficient (0.23), the highest ME (-220.29), and RMAE (-0.145).

Among the three satellite rainfall estimates evaluated based on observed gauge stations, TAMSAT-V3.1 scored the best Nash-Sutcliffe Efficiency coefficient (0.321), which indicates the best skill of the estimates relative to the gauge mean. In contrast, PERSIANN-CDR had the poorest value of the Nash-Sutcliffe Efficiency Coefficient, with a value of –1.361.

The bias indicates how well the mean estimate and gauge mean correspond. As the perfect score is 1, CHIRPS-V2 had a 1.01, TAMSAT-V3.1 had 0.98, and PERSIANN-CDR had the lowest bias of 0.84. In terms of annual rainfall estimation, CHIRPS-V2 is better at overestimating the observed rainfall, which can be important for flood monitoring, whereas PERSIANN-CDR is the poorest dataset that underestimates the observed value of rainfall, which indicates the dataset could be a better source of data for drought monitoring than flood monitoring. This result is in line with the findings of Dinku et al. (2018) which indicated that CHIRPS-V2 outperforms the latest version of TAMSAT in annual rainfall estimation.

Table 9: the continuous statistical verification for the Annual rainfall analyzed in *Gumera* Watershed from 2004-2019

Dataset	*r*	*ME*	*RMAE*	*Eff*	*BIAS*
CHIRPS-V2	0.62	26.19	0.017	- 0.036	1.01
TAMSAT-V3.1	0.74	-19.68	- 0.013	0.321	0.98
PERSIANN-CDR	0.23	-220.29	- 0.145	-1.361	0.84

Highest lowest

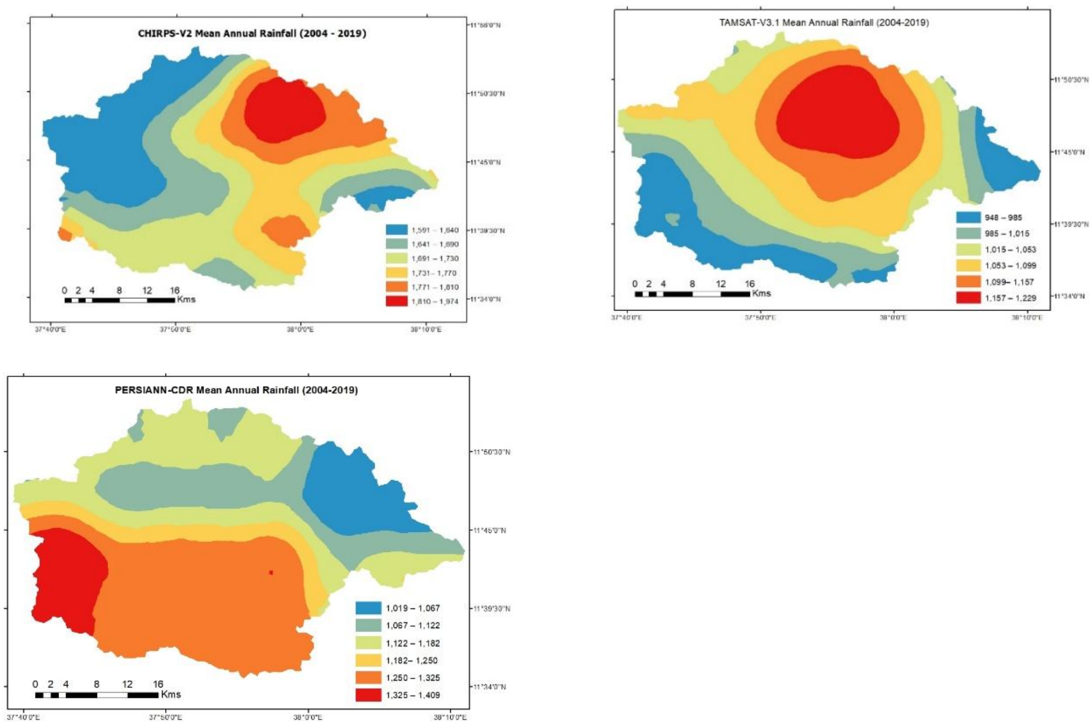

Figure 7: CHIRPS-V2, TAMSAT-V3.1 and PERSIANN-CDR Mean Annual Rainfall from 2004 - 2019

As indicated in figure 7, the mean annual rainfall estimates by CHIRPS-V2, TAMSAT-3.1 and PERSIANN-CDR had almost similar patterns, with the highest amount of rainfall in the east and northeastern sections of the watershed. These patterns have a positive association with the elevation of the area that increased from west to east directions, which indicates a positive correlation with the elevation and slope of the watershed.

As depicted in Figure 8 the watershed's topography can be divided into two categories. The upper parts of the watershed are mountainous, but the lower parts are quite flat and moderate, with a general west-to-east slope. The watershed's slope is indicated in the map below on Figure 8.

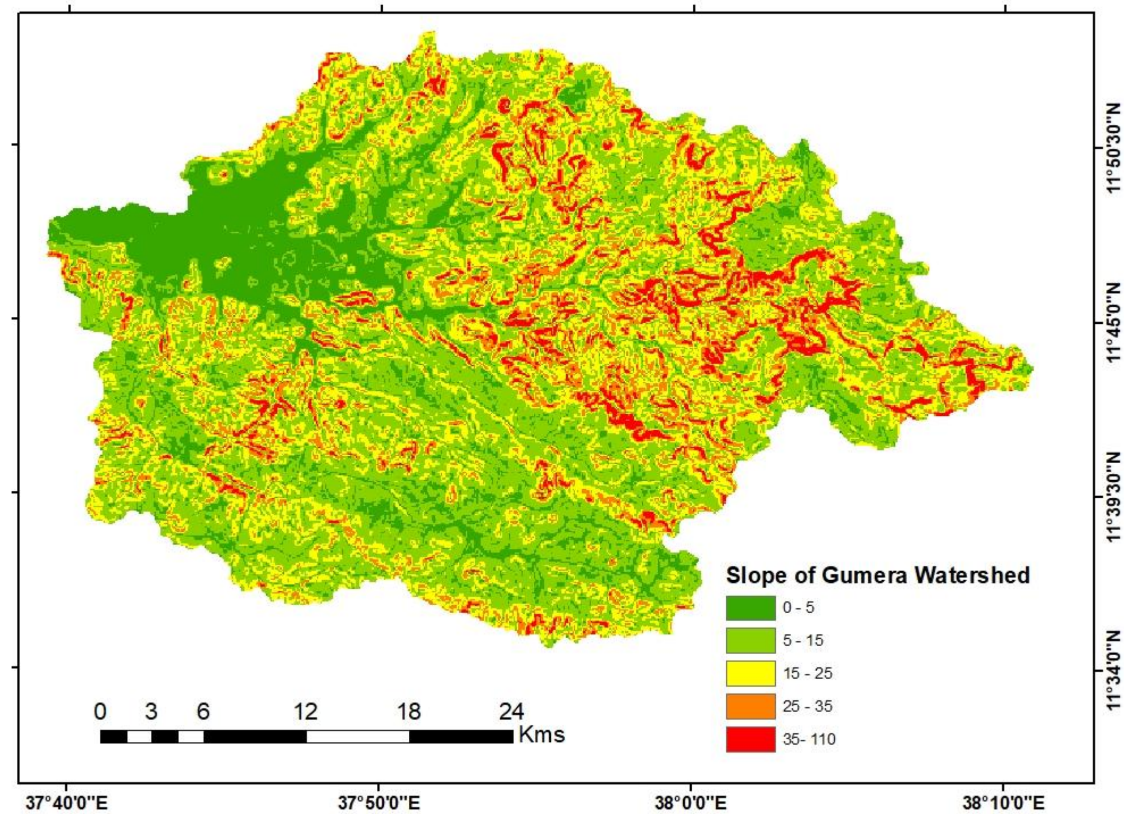

Figure 8: Slope Map of *Gumera* Watershed

4.2.2. Seasonal Rainfall Evaluation

The other performance evaluation of satellite rainfall estimates is considering the mean amount of the four months of rainfall (seasonal) observed by the rain gauge stations. These amounts of rainfall can be considered the wettest season rainfall in the study area obtained from the monthly satellite estimates. The observed and estimated mean seasonal rainfall is indicated in the following table.

Table 10: *Kiremt* season average rainfall (mm) of *Gumera* Watershed from 2004 to 2019

Year	**Gauge**	**CHIRPS**	**TAMSAT**	**PERSIANN-CDR**
2004	898.7	976.77	958.87	839.46
2005	1279.78	1072.49	1168.12	782.36
2006	1350.2	1268.12	1137.86	956.05
2007	1364.38	1126.87	1177.36	867.10
2008	1299.12	1142.00	1187.70	798.36
2009	1100.74	871.28	1010.16	665.99
2010	1329.26	1171.95	1519.42	1003.04
2011	1242.54	1056.05	1152.70	769.56
2012	1387.3	1222.30	1271.82	789.91
2013	1376.52	1160.29	1207.68	764.94
2014	1153.44	1006.23	1016.76	786.76
2015	1168.76	906.70	1084.54	750.46
2016	1071.6	1098.71	1116.60	718.97
2017	1031.22	1196.17	1285.10	812.79
2018	1311.62	1141.17	1117.12	931.12
2019	1245.08	1275.24	1130.70	832.08

Source: NMA (2022), https://www.chc.ucsb.edu/data, http://www.TAMSAT-V3.1.org.uk/data/ and https://chrsdata.eng.uci.edu/

As depicted in Table 10, the gauge measurement recorded the highest seasonal rainfall in 2012 with a value of 1387.3 mm. whereas CHIRPS-V2 estimated the highest rainfall in 2019 with 1275.24 mm, and both TAMSAT-V3.1 and PERSIANN-CDR estimated the highest rainfall in 2010 with 1519.42 mm and 1003.04 mm, respectively. The table also shows the lowest measurement of *kiremt* season observed and estimated rainfall using the gauge stations and the three satellite datasets. The lowest wet season rainfall was observed in 2004 with 898.7 mm. Similarly, TAMSAT-V3.1 also estimated the lowest wet season rainfall in 2004 with 958.87 mm, whereas CHIRPS-V2 and PERSIANN-CDR estimated the lowest amount of rainfall in 2009 with 871.28 mm and 665.99 mm, respectively.

The performance of satellite rainfall estimates during the *kiremt* season of the study area was evaluated using continuous statistical indices. Table 11 shows the continuous statistical verifications of the wet season mean rainfall from 2004 to 2019.

Table 11: the continuous statistical verification for the Wet season rainfall analyzed in *Gumera* Watershed from 2004-2019

Dataset	*r*	*ME*	*RMAE*	*Eff*	*BIAS*
CHIRPS-V2	0.54	-124.2	-0.10	-0.72	0.90
TAMSAT-V3.1	**0.55**	**-77.8**	**-0.06**	**-0.22**	**0.94**
PERSIANN-CDR	0.47	-400.4	-0.32	-9.36	0.67

Highest lowest

As depicted in Table 11, similar to the annual rainfall estimation, the TAMSAT-V3.1 seasonal rainfall estimation had better agreement with the observed amount of rainfall, with the highest correlation coefficient (r), lower mean error (ME) and root mean absolute error (RMAE) and Bias nearest to 1. The seasonal estimation of TAMSAT-V3.1 had a correlation coefficient of 0.55, ME of -77.8, RMAE of -0.06, and Bias of 0.94.

CHIRPS-V2 also had almost similar correlation coefficient with TAMSAT-V3.1 (0.54), which indicates this dataset had also relatively better at estimating the mean seasonal observed rainfall amount. PERSIANN-CDR had poor performance in estimating the amount of observed rainfall on a seasonal temporal scale. This finding is parallel with the findings of Yared et al. (2017) indicated that CHIRPS-V2 is better than PERSIANN-CDR in estimating the observed seasonal rainfall.

4.2.3. Monthly Rainfall Evaluation

The months considered for this performance evaluation of the satellite rainfall estimate are the four major rainy months of the watershed; including June, July, August, and September. These are the months when maximum rainfall was observed in the country in general and the study area in particular. In these processes, evaluation was conducted based on four classes by considering the four months; June, July, August, and September. The following figure shows the rainfall conditions for the four months from 2004-2019 in *the Gumera* watershed.

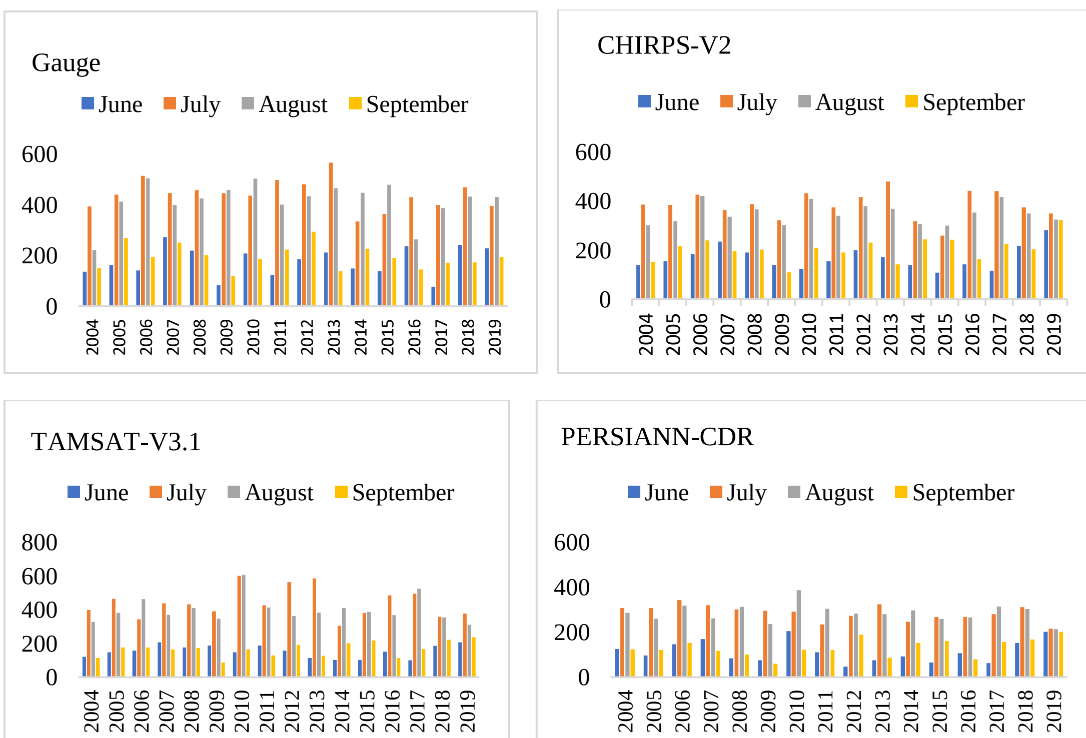

Figure 9: Monthly rainfall (Gauge, CHIRPS-V2, TAMSAT-V3.1 and PERSIANN-CDR) of *Gumera* watershed from 2004 to 2019

Source: NMA (2022), https://www.chc.ucsb.edu/data, http://www.TAMSAT-V3.1.org.uk/data/ and https://chrsdata.eng.uci.edu/

Figure 9 shows the rainfall pattern during the four rainy months in *the Gumera* watershed from 2004 to 2019. According to the measured data collected from the National Meteorological Agency, the highest rainfall in June was recorded in 2007 with a value of 271.6 mm, followed by 2018 and 2016 with 241.2 mm and 235.8 mm, respectively. The data collected from the CHIRPS-V2 dataset showed that the highest rainfall during the study period of June was estimated in 2019 with 280.9 mm, followed by 2007 and 2018 with 234.5 mm and 216 mm, respectively. During the same month, both TAMSAT-V3.1 and PERSIANN-CDR datasets estimated the highest rainfall in 2019 with 206.6mm and 201.4mm, respectively. According to TAMSAT-V3.1, the second highest rainfall estimate was in 2007 with 206.2 mm, whereas, PERSIANN-CDR dataset estimates 2010 as the second highest rainfall period with 204.8 mm.

In the study area, during June the lowest rainfall was observed by the gauge stations in 2017 with 76.3mm followed by 2009 with 82.1mm. TAMSAT-V3.1 estimated the lowest rainfall of the month in 2007 with 99.8mm followed by 2015 with 100.9mm. According to CHIRPS-V2 and PERSIANN-CDR rainfall dataset, the lowest rainfall in June was estimated in 2015 and 2012 at 107.1mm and 46.7mm respectively.

During July, the highest observed rainfall was recorded in 2006 with 502.6mm followed by 2011 and 2012 with 496.5 mm and 478 mm respectively. PERSIANN-CDR also estimated the highest rainfall of the month in 2006 with a value of 341mm. However, CHIRPS-V2 and TAMSAT-3.1 estimated the highest amount of rainfall of the month in 2013 and 2010 with 478.2 mm and 600.3 mm respectively. Regarding the lowest rainfall of July, the observed amount of rainfall and TAMSAT-V3.1 were estimated in 2014 as

333.3 mm and 305.2 mm respectively. Whereas, CHIRPS-V2 and PERSIANN-CDR rainfall datasets estimated the lowest amount of rainfall during 2015 and 2019 with 258.4 mm and 216.2 mm respectively.

Concerning the amount of rainfall in August during the study period, CHIRPS-V2 estimation is parallel with the observed amount of rainfall, which was recorded as 502.6mm in 2006 with a value of 420.1mm whereas, TAMSAT-V2 and PERSIANN-CDR rainfall datasets estimated the highest amount of monthly rainfall in 2010 with 606.3mm and 385.5 mm respectively. Similarly, the two satellite datasets also estimate the lowest month of rainfall in 2019. According to the dataset of TAMSAT-V2 and PERSIANN-CDR, in the study period, the lowest rainfall of August was estimated with a value of 310.6mm and 212.4mm respectively. Differently, the lowest amount of August rainfall was observed in 2014 with 220.5 mm, which was estimated as 300.1 mm by the CHIRPS-V2 dataset.

Regarding the rainfall amount of September, all the three satellites estimate the highest amount of rainfall in 2019 (CHIRPS-V2, 322.8 mm; TAMSAT-V3.1mm, 236.1 mm and PERSIANN-CDR, 201.9 mm.), whereas the highest observed amount of rainfall was recorded in 2012 with 292.5 mm followed by 2005 with 267.4 mm. Concerning estimating the lowest rainfall of September, the estimation of the three satellites was parallel with the observed amount. Accordingly, the lowest amount of rainfall was observed and estimated in 2009 (Gauge measurement, 117.3 mm; CHIRPS-V2, 109.2 mm; TAMSAT-V3.1, 87.1 mm and PERSIANN-CDR, 59.7 mm).

The performance of the three satellites in estimating the monthly rainfall observed in the study area was evaluated using both continuous statistical indices and categorical verification statistics using the daily rainfall of each month. Table 11 showed the continuous statistical indices result of the three satellite datasets for each month of the rainy season.

Table 12: the continuous statistical verification for the monthly rainfall analyzed in *Gumera* Watershed from 2004-2019

Con. Stat. Indices	Dataset and Month											
	CHIRPS-V2				TAMSAT-V3.1				PERSIANN-CDR			
	June	July	August	Sept.	June	July	August	Sept.	June	July	August	Sept.
r	**0.64**	**0.62**	0.28	**0.49**	0.44	0.43	**0.38**	0.48	0.51	0.49	0.21	0.47
ME	**-6.9**	-56.8	-66.6	**10.4**	-22.3	**-0.8**	-14.7	-28.7	-62.2	-154.3	-129.3	-62.9
RMAE	-0.04	-0.13	-0.16	0.05	-0.13	-0.001	-0.03	-0.15	-0.35	-0.35	-0.31	-0.32
Eff	0.37	-0.75	-0.79	-3.54	-0.00003	-0.96	-0.26	-0.32	-1.08	-7.35	-3.1	-1.72
BIAS	**0.96**	0.87	0.83	**1.05**	0.87	**0.99**	**0.96**	0.85	0.64	0.64	0.68	0.67

Highest lowest

Table 12 showed that, the performance of the three-satellite rainfall dataset in estimating the rain gauge observations from 2004 to 2019 at a monthly temporal scale. As it is indicated in the table, CHIRPS-V2 had a better agreement with the June, July, and September rainfall observations with the highest correlation coefficients of 0.64, 0.62, and 0.49 better Bias and lower ME and RMAE (r = 0.64, Bias = 0.96, ME = -6.9 and RMAE = -0.04). Similarly, PERSIANN-CDR had also better agreement during June with r value of 0.51. Whereas, TAMSAT-V3.1 had a better agreement with the observed rainfall data during August with a correlation coefficient (r) value of 0.38.

In estimating the monthly rainfall, the mean estimate of TAMSAT-V3.1 was better during July and August with values of 0.99 and 0.96. CHIRPS-V2 also had a good mean estimate with the observed data during June with a Bias value of 0.96. Moreover, CHIRPS-V2 had almost perfect Bias during September with 1.05. Whereas, relative to TAMSAT-V3.1 and CHIRPS-V2 in estimating the mean of the observed rainfall PERSIANN-CDR satellite rainfall dataset had poor performance. Yared et.al (2017) also approved that, CHIRPS-V2 had better performances than PERSIANN-CDR in monthly temporal scale.

The performances of the satellite rainfall datasets were also evaluated using categorical verification statistics. The following figure showed the Probability of detection (*PoD*), False alarm Ratio (*FAR*), and Critical success index (*CSI*) of the daily rainfall during the four months of *Kiremt* season.

Table 13: the categorical verification statistics for the monthly rainfall analyzed in *Gumera* Watershed from 2004-2019

Categorical Evaluation Statistics	Dataset and Month											
	CHIRPS-V2				TAMSAT-V3.1				PERSIANN-CDR			
	June	July	August	Sept.	June	July	August	Sept.	June	July	August	Sept.
PoD	0.87	0.94	0.96	0.88	0.87	0.95	0.97	0.87	0.85	0.97	0.99	0.89
FAR	0.13	0	0.006	0.13	0.16	0	0.008	0.12	0.15	0	0.008	0.11
CSI	0.73	0.94	0.95	0.78	0.74	095	0.96	0.78	0.73	097	0.98	0.80

Highest Lowest

Table 13, showed the categorical statistical comprises critical success index, false alarm ratio and probability of detection. The result of probability of detection and critical success index nearer to one indicates the highest detecting capacity of the satellites. Except for June, PERSIANN-CDR had the highest capacity of detection (July = 0.97, August = 0.99, and September =0.89 than CHIRPS-V2 and TAMSAT-V3.1 satellite rainfall dataset. CHIRPS-V2 and TAMSAT-V3.1 satellite rainfall dataset had similar detecting capacity during June with 0.87.

Regarding the false alarm ratio, all the three satellite rainfall datasets had similar capacity during July with a perfect score, which is zero. In the remaining three months, CHIRPS-V2 had the lowest value of FAR during June and August, while PERSIANN-CDR had the lowest FAR during September with 0.11. PERSIANN-CDR had also the highest critical success index during the three months except for June.

4.2.4. Daily Rainfall Evaluation

The observed daily rainfall of the *kiremt* season from 2004 to 2019 was used to evaluate the daily estimates of the rainfall. Hence, the daily estimated rainfall was compared with the daily observed rainfall collected from the national meteorological agency. The performance evaluation was conducted by using both continuous and categorical statistical indices. The results of continuous statistical indices are indicated in the following table.

Table 14: the continuous statistical verification for the daily rainfall analyzed in *Gumera* Watershed from 2004-2019

Dataset	r	ME	RMAE	*Eff*	BIAS
CHIRPS-V2	0.49	-1.3	-0.13	0.03	0.88
TAMSAT-V3.1	0.59	-0.3	-0.03	0.20	0.96
PERSIANN-CDR	0.53	-4.0	-0.39	0.09	0.66

Highest Lowest

Table 14 presents the overall evaluation of the daily satellite rainfall estimates of the study period against the observed daily rainfall data. As the table showed, concerning the daily rainfall estimate TAMSAT-3.1 showed better agreement with the rain gauge data with a correlation coefficient (r) value of 0.59 followed by PERSIANN-CDR with a correlation coefficient (r) of 0.53. This result is parallel with Dinku et al., (2018) findings that approved TAMSAT-V3.1 had better skill to estimate the daily rainfall of the gauge observation.

Table 14 also showed the ME and RMAE value of the three satellite datasets. The lower value of the mean error and root mean absolute error shows the lower average estimation error of the satellite datasets against the observed rainfall. TAMSAT-V3.1 had a better accuracy with the lowest ME and RMAE followed by CHIRPS-V2 with values of -0.3, -0.03, -1.3, and -0.13 respectively. PERSIANN-CDR satellite dataset had the highest mean error and root mean absolute error with -408 and -0.33 respectively, which reflects a higher average estimation error.

The Nash-Sutcliffe efficiency coefficient (Eff) and Bias of the three-satellite dataset are also indicated on Table14. *Eff* shows the skill of the estimates relative to the gauge means and the perfect score is 1. TAMSAT-V3.1 had relatively the best score to the gauge mean with a value of 0.20 followed by PERSIANN-CDR and CHIRPS-V2 with a value of 0.09 and 0.03 respectively.

Bias shows how well the mean estimate and gauge mean to correspond with a perfect score of 1. The Bias of the three-satellite dataset was 0.96, 0.88, and 0.66 for TAMSAT-V3.1, CHIRPS -V2 and PERSIANN-CDR respectively. These show the mean estimate of TAMSAT-V3.1 and gauge mean corresponded in a better way followed by the mean estimate of CHIRPS-V2 while PERSIANN-CDR had the lowest bias values of 0.66. The correlation coefficient (r) of the three-satellite dataset is illustrated in the following scatter plot graphic.

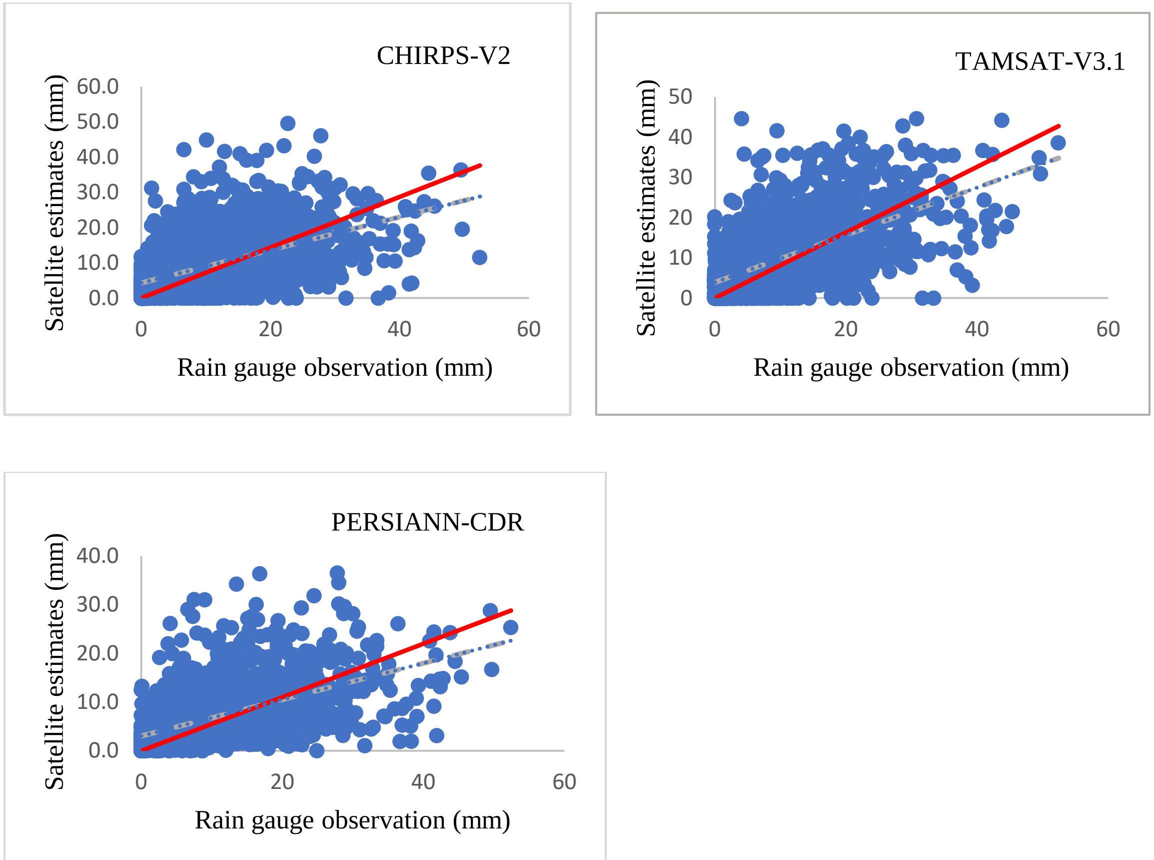

Figure 10: comparison of daily rainfall between rain gauge observations versus the three satellite-based rainfall estimates (N = 1952) from 2004-2019 using scatter plots. The 1:1 correspondence is indicated by dashed line and red line gives the linear regression best fit.

Table 15: the categorical verification statistics for the daily rainfall analyzed in *Gumera* Watershed from 2004-2019

Dataset	*PoD*	*FAR*	CSI
CHIRPS-V2	0.92	0.069	0.86
TAMSAT-V3.1	0.92	0.063	0.87
PERSIANN-CDR	0.94	0.059	0.88

Highest Lowest

The categorical findings of the statistical analysis on daily observed rainfall with the estimated satellite rainfall are indicated in Table 15. CHIRPS-V2 and TAMSAT-V3.1 satellite rainfall dataset had similar quality in the probability of detection (PoD) with a value of 0.92, which means 92 percent of the observed rainfall is correctly detected. PERSIANN-CDR had the best quality to detect the daily observed rainfall with a value of 0.94. Similarly, CHIRPS-V2 and TAMSAT-V3.1 had almost similar false alarm ratios and critical succus index. The FAR value of the two satellite datasets is 0.069 and 0.063, which indicates there was approximately 7 percent of a false alarm that estimates the availability of rainfall which was wrong in the daily observed rainfall. Similar to the detecting capacity, PERSIANN-CDR is a good satellite dataset with a lower false alarm ratio of 0.059.

CHIRPS-V2, TAMSAT-V3.1, and PERSIAN-CDR had a critical success index of 0.86, 0.87, and 0.88 respectively concerning the daily observed rainfall between 2004 and 2019. These indicates PERSIANN-CDR had good quality followed by CHIRPS-V2 and TAMSAT-V3.1. Therefore, it is possible to conclude that concerning the highest probability of detection, higher critical success index, and lower false alarm ratio PERSIANN-CDR had better quality than the two datasets, whereas, CHIRPS-V2 and TAMSAT-V3.1 had a similar capability.

4.3. Evaluation of Satellite Rainfall Estimates for Flood Monitoring

To check the performance of the satellite rainfall datasets for flood monitoring, two types of specific performance evaluations were employed. First, an evaluation was conducted for the whole observed and estimated daily rainfall of the study area during the study period. Second, the evaluation was conducted based on the occurrences of flood events from 2004 to 2019. In this processes rainfall category were developed to check the capabilities of the satellites in estimating the lowest and highest rainfall of the area which is important to check the capability of the satellites in estimating rainfall during the occurrences of flood.

4.3.1. Evaluation of SRE on Daily Basis

One of the most important methods used to check the performances of satellite rainfall datasets for flood monitoring is testing per daily rainfall category (Tote et al., 2015). Based on the observed rainfall data collected from the national meteorological agency and Tote et al., (2015) recommendations, eight categories of rainfall data were developed. These include rainfall below 5 mm (N=588), 5-10 mm (N=496), 10-15 mm (N=391), 15-20 mm (N=236), 20-25 mm (N=123), 25-30 mm (N=59), 30-35 mm (N=27), and above 35 mm (N=27). The distribution of the observed and estimated data per the above-stated rainfall category is indicated in Figure 11.

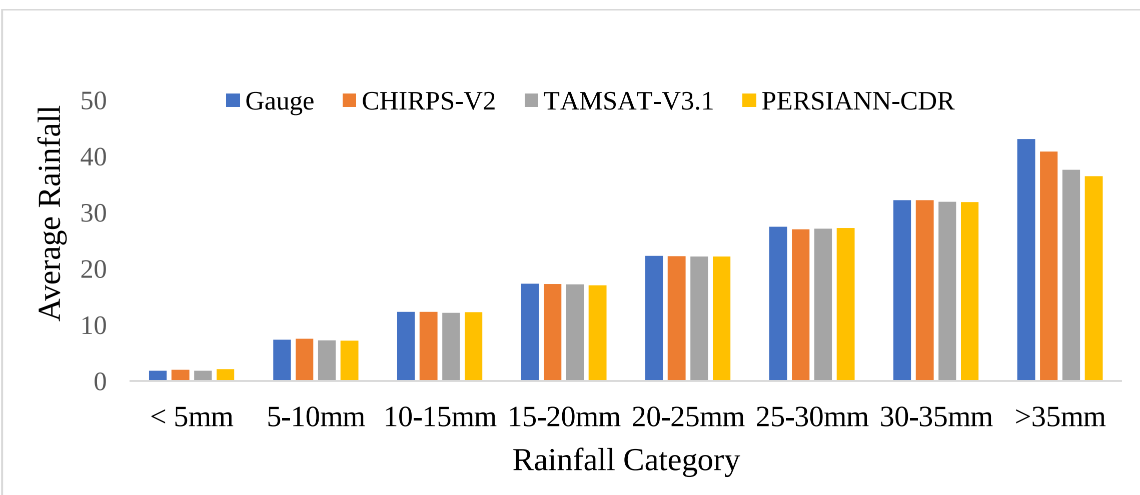

Figure 11: Rainfall Distribution per Category

Figure 11 showed that the estimated rainfall had a better agreement in estimating the lowest amount of rainfall observed per day. The average observed amount of rainfall in the first category is 1.82, which is overestimated by PERSIANN-CDR and CHIRPS-V2 as 2.12 and 1.98 respectively. Hence, it is possible to conclude that in the lowest amount of observed rainfall the two-satellite dataset overestimates the amount of rainfall which is recommended for drought monitoring. This result is parallel with the findings of Toté et al., (2015). TAMSAT-V3.1 had a relatively similar estimation with the observed rainfall data as 1.8.

For effective flood monitoring, a satellite dataset that overestimates the highest amount of rainfall is recommended. Figure 11 indicated that, in the highest rainfall category (above 35) all the three satellites underestimate the amount of observed rainfall in *Gumera* watershed. The average observed rainfall amount found in the last category (above 35), was 43.06 and CHIRPS-V2 is relatively better in estimating the highest rainfall amount as 40.85 followed by TAMSAT-V3.1 estimation as 37.59. PERSIANN-CDR had poor capacity in estimating the highest amount of rainfall with a value of 36.42 which is parallel with the findings of Li et.al (2013). Therefore, it is possible to conclude that, CHIRPS-V2 is better at monitoring floods than the two satellites in the study area. This is parallel with the findings of Tote et.al (2015) which indicates CHIRPS performs well in estimating the highest amount of rainfall.

Continuous statistical indices were also employed to evaluate the performances of the three-satellite rainfall estimates against the observed data collected from the Ethiopian National Meteorological Agency from 2004 to 2019.

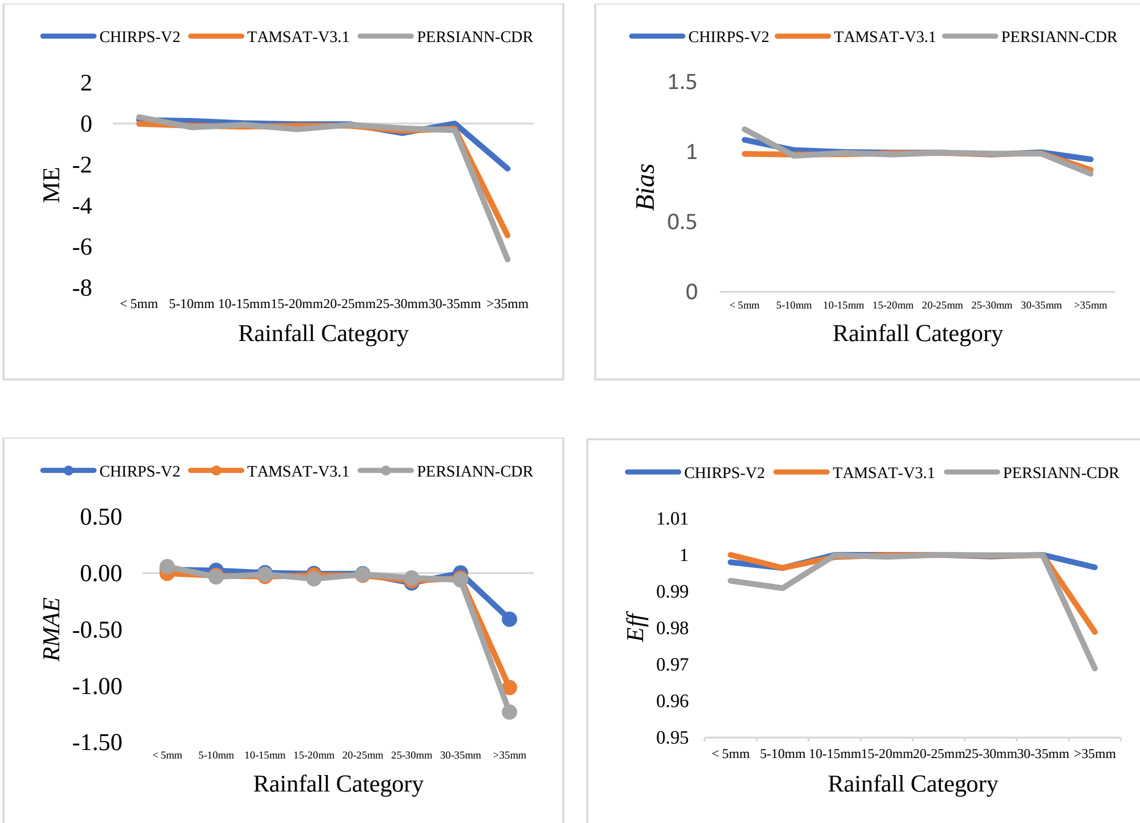

Figure 12: Continuous statistical indices (ME, RMAE, Eff and Bias) of the satellite datasets compared to the mean observed rainfall in the specified category. The straight line indicates the perfect score.

As figure 12 indicates, the three satellites had a good performance in estimating the lowest amount of rainfall with ME and RMAE values nearest to zero and *Eff* and Bias values nearest to one. However, in estimating the highest amount of rainfall (above 35 mm), all the three satellites underestimate the observed rainfall data. In comparison, CHIRPS-V2 had a good performance with the lowest ME and RMAE and relatively better Bias and *Eff* values. Therefore, it is possible to conclude that CHIRPS-V2 is a dataset that had better performance for flood monitoring in the study area from 2004 to 2019.

4.3.2. Evaluation of SRE during Flood Events

According to the *Fogera woreda* Agricultural office, major flood events were occurred in three different years during the stated study period. These include 2006, 2017, and 2019 and the flood occurred during the two rainy months of the country (July and August). To evaluate the performances of the satellite rainfall products for flood monitoring, eight rainfall categories were developed (below 5mm, 5-10 mm, 10-15 mm, 15-20 mm, 20-25 mm, 25-30 mm, 30-35 mm, and above 35 mm). This category helps to check the performances of the satellites in detecting the highest rainfall observed in the stated area during the flooding time. Figure 13 indicates the distribution of observed rainfall in 2006, 2017, and 2019.

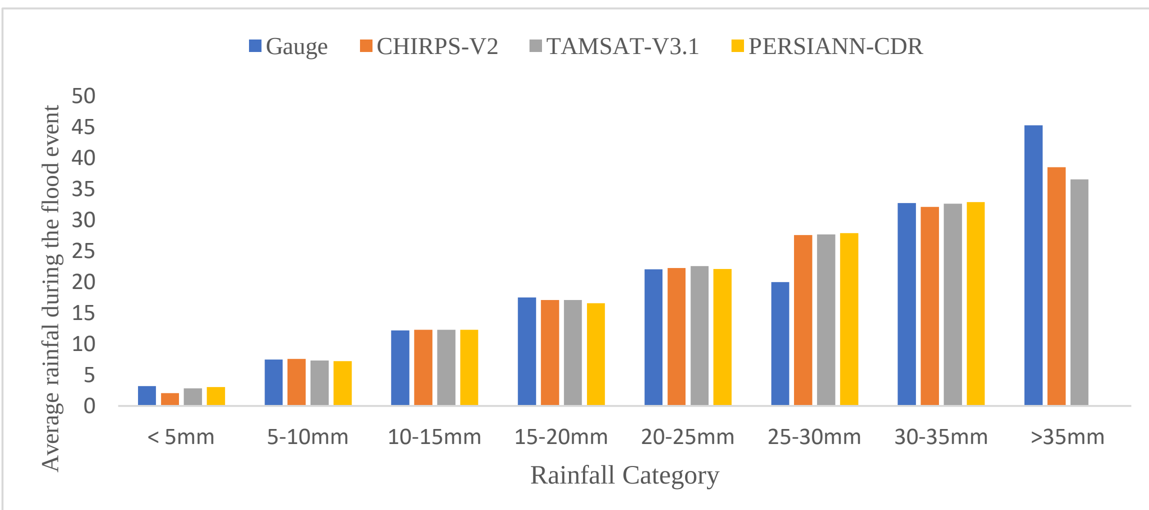

Figure 13: Average observed and estimated rainfall distribution under rainfall category during the flood events of (2006, 2017 and 2019)

As depicted in figure 13, the satellite rainfall dataset had better performances in detecting the lowest amount of rainfall. In estimating the highest amount of rainfall which could be the cause for the occurrences of flood events in the study area, CHIRPS-V2 had better performance followed by TAMSAT-V3.1. PERSIANN-CDR had poor performance in estimating the highest amount of rainfall. This is indicated by the last category of rainfall (above 35mm), which is not captured by the PERSIANN-CDR dataset. Therefore, CHIRPS-V2 had a good quality to monitor floods than the two satellite datasets in the study area.

In addition to the average rainfall identified by different rainfall categories, the performances of the three-satellite data were also evaluated using continuous statistics. The following table shows the results of continuous statistical indices (r, ME, RMAE, and Bias) of 2006, 2017, and 2019 July and August month daily rainfall.

Table 16: The Continuous statistical indices of daily rainfall during the months of July and August in 2006, 2017 and 2019 in *Gumera* watershed

Dataset	r	ME	RMAE	*Eff*	BIAS
CHIRPS-V2	0.31	-0.76	-0.05	-0.36	0.95
TAMSAT-V3.1	0.52	-0.54	-0.03	0.11	0.96
PERSIANN-CDR	0.44	-4.76	-0.33	-0.12	0.66

Highest Lowest

Table 16 showed that TAMSAT-V3.1 had a correlation coefficient of 0.52 followed by PERSIANN-CDR and CHIRPS-V2 with r values of 0.44 and 0.31. This indicates that TAMSAT-V3.1 had a better association with the observed data during the occurrences of flood events. However, CHIRPS-V2 is the best satellite during the time of flood occurrences in estimating the gauge means than TAMSAT-V3.1 and PERSIANN-CDR, which have almost similar Bias values with the daily rainfall estimates.

Generally, based on the distribution of daily rainfall during the time of flood and the results of continuous statistical indices CHIRPS-V2 satellite rainfall dataset had a better skill to estimate the observed rainfall in the study area.

Chapter Five

5. Conclusion and Recommendation

5.1. Conclusion

The performance of the three satellite rainfall datasets, including CHIRPS-V2, TAMSAT-V3.1, and PERSIANN-CDR, was evaluated against the ground-based data gathered from the Ethiopian National Meteorological Agency. This data has been evaluated on the annual, seasonal, monthly, and daily temporal scales in one of the most flood-prone areas of Amhara Region, Ethiopia. The ground-based data was collected from the stations found in and near the watershed for sixteen years (2004–2019). The data indicates that there was continuous variability in rainfall during the stated research period.

On the annual temporal scale, TAMSAT-V3.1 had better agreement with the rain gauge measurement, with the highest correlation coefficient, lower ME, and RMAE, followed by CHIRPS-V2. PERSIANN-CDR had a poor agreement with the observed data with the lowest correlation coefficient, the highest ME, and RMAE. Similarly, TAMSAT-V3.1 had the better skill of the estimates relative to the gauge mean, with the best score in the Nash-Sutcliffe Efficiency coefficient (Eff). Whereas, PERSIANN-CDR had the lowest value in the Nash-Sutcliffe Efficiency Coefficient (Eff). In terms of the correspondence between the estimated and gauge mean, CHIRPS had the better skill, with a bias value nearest to the perfect score. While PERSIANN-CDR had the lowest value of bias.

In terms of seasonal temporal scale, both TAMSAT-V3.1 and CHIRPS-V2 had better agreement with the observed amount of rainfall with a relatively similar correlation coefficient, whereas, PERSIANN-CDR had poor performance in estimating the amount of observed rainfall. Regarding the monthly rainfall evaluation, CHIPRS-V2 had better agreement with the monthly observed rainfall with the highest correlation coefficients, better bias, and lower ME and RMAE. In the categorical statistics, PERSIANN-CDR has the highest capacity of detection than CHIRPS-V2 and TAMSAT-V3.1 satellites.

The evaluation of the satellite rainfall products for flood monitoring results shows that satellite estimates overestimate lower daily rainfall values and underestimate higher values, which could be the causes of flood occurrences. In comparison, CHIRPS-V2 outperformed TAMSAT-V3.1 and PERSIANN-CDR in detecting the highest amounts of daily rainfall in the study area. These were also approved by the evaluation made during the flooding times of 2006, 2017, and 2019 in the *Gumera* watershed of the Amhara region.

5.2. Recommendation

All the three-satellite rainfall datasets evaluated by this study showed good qualities and shortcomings when applied for flood monitoring. Therefore, further research should be conducted on how to improve the qualities of the satellite datasets by reducing the observed shortcomings. Moreover, researchers should evaluate and make required calibrations for the rainfall values derived from the satellite products before being applied to different hydrological research.

This study only evaluates the performances of CHIRPS-V2, TAMSAT-V3.1, and PERSIANN-CDR satellite rainfall estimates during the occurrences of rainfall. But the study could not address when and where the flood will occur (flood prediction). Hence, a comprehensive study should be conducted on the prediction of flood events in *Gumera* watershed and other flood-prone areas of Amhara region in particular and Ethiopia in general, using different satellite-based rainfall estimates and hydrologic models in conjunction with ground-based rainfall observations.

References

Alhamshry, Fenta, Shimizu, Yasuda, and Kimura. (2020). "*Seasonal Rainfall Variability in Ethiopia and Its Long-Term Link to Global Sea Surface Temperatures*." Water 2020, 12, 55; doi:10.3390/w12010055: www.mdpi.com/journal/water.

Alijanian, M, Rakhshandehroo, G. R, Mishra, A. K and Dehghani, M. (2019). "*Evaluation of satellite rainfall climatology using CMORPH, PERSIANN-CDR, PERSIANN, TRMM, MSWEP over Iran*", international journal of climatology Int. J. Climatol. (2017) Published online in Wiley Online Library (wileyonlinelibrary.com) DOI: 10.1002/joc.5131.

Ayehu, G. T., Tadesse, T., Gessesse, B., and Dinku, T. (2018). *Validation of new satellite rainfall products over the Upper Blue Nile Basin , Ethiopia*. 1921–1936.

Bai, L., Shi, C., Li, L., Yang, Y., & Wu, J. (n.d.). *Accuracy of CHIRPS Satellite-Rainfall Products over*. https://doi.org/10.3390/rs10030362

Belay, A. S., Fenta, A. A., Yenehun, A., Nigate, F., Tilahun, S. A., Moges, M. M., Dessie, M., Adgo, E., Nyssen, J., Chen, M., Griensven, A. Van, & Walraevens, K. (2019). *Evaluation and Application of Multi-Source Satellite Rainfall Product CHIRPS to Assess Spatio-Temporal Rainfall Variability on Data-Sparse Western Margins of Ethiopian Highlands*. 1–22.

Bewket, W. (2009). *Rainfall variability and crop production in Ethiopia Case study in the Amhara region*. 823–836.

Cantero, F. N. (2017). *Spatial and Trend Analyses of Rainfall Seasonality and Erosivity in the West of Andalusia (Period*. *182*(4), 1–13. https://doi.org/10.1097/SS.0000000000000206

Chiaravalloti, F., Brocca, L., Procopio, A., Massari, C., & Gabriele, S. (2022). *Assessment of GPM and SM2RAIN-ASCAT rainfall products over complex terrain in southern Italy.* Atmospheric Research, 206 (December 2017), 64–74. https://doi.org/10.1016/j.atmosres.2018.02.019

Darand, M., & Siavashi, Z. (2021). *An evaluation of Global Satellite Mapping of Precipitation (GSMaP) datasets over Iran*. Meteorology and Atmospheric Physics, *133*(3), 911–923. https://doi.org/10.1007/s00703-021-00789-y

Dembélé, M., & Zwart, S. J. (2016). *Evaluation and comparison of satellite-based rainfall products in Burkina Faso* , West Africa. International Journal of Remote Sensing, *37*(17), 3995–4014. https://doi.org/10.1080/01431161.2016.1207258

Dinku, T., Funk, C., Peterson, P., Maidment, R., & Tadesse, T. (2018). *Validation of the CHIRPS satellite rainfall estimates over eastern*. *June 2017*, 292–312. https://doi.org/10.1002/qj.3244

Fink, A. H., Funk, C., & Pinto, J. G. (2021). *Using seasonal rainfall clusters to explain the interannual variability of the rain belt over the Greater Horn of Africa*. *41*(September 2020), 1717–1737. https://doi.org/10.1002/joc.6802

Funk, C., Peterson, P., Landsfeld, M., Pedreros, D., Verdin, J., Shukla, S., Husak, G., Rowland, J., Harrison, L., Hoell, A., & Michaelsen, J. (2015). *The climate hazards infrared precipitation with stations — a new environmental record for monitoring extremes*. 1–21. https://doi.org/10.1038/sdata.2015.66

Hu, Q., Li, Z., Wang, L., Huang, Y., Wang, Y., & Li, L. (n.d.). *Rainfall Spatial Estimations : A Review from Spatial Interpolation to Multi-Source Data Merging*. 1–30. https://doi.org/10.3390/w11030579

Karam A. Elzopy, Ashish K. Chaturvedi, K. Madhava Chandran, Girish Gopinath, Naveena K and U. Surendran. (2020). *Trend analysis of long-term rainfall and temperature data for Ethiopia*, South African geographical journal, https://doi.org/10.1080/03736245.2020.1835699

Kyaw, K. A. Y. K. (2020). *Validation Of Satellite Datasets For The Operation Of Flood And Drought Indicators In Certain Regions of Myanmar*. 1–8.

Li xianghu, Zhang Qi and Yu Xu Xhong. (2013). *Assessing the performance of satellite-based precipitation products and its dependence on topography over Poyang Lake basin,* Theor Appl Climatol (2014) 115:713–729, DOI 10.1007/s00704-013-0917-x

Maidment, R. I., Grimes, D., Black, E., Tarnavsky, E., Young, M., Greatrex, H., Allan, R. P., Stein, T., Nkonde, E., Senkunda, S., Misael, E., & Alcántara, U. (2017). *Data Descriptor : A new , long-term daily satellite-based rainfall dataset for operational monitoring in Africa*. Nature Publishing Group. https://doi.org/10.1038/sdata.2017.63

Mekonen, A. A. (2021). *Rural households ' livelihood vulnerability to climate variability and extremes : a livelihood zone-based approach in the Northeastern Highlands of Ethiopia*.

Mekonnen, K., Melesse, A. M., & Ayele, T. (2022). *How suitable are satellite rainfall estimates in simulating high fl ows and actual evapotranspiration in MelkaKunitre catchment* , Upper Awash Basin , Ethiopia ? Science of the Total Environment, *806*, 150443. https://doi.org/10.1016/j.scitotenv.2021.150443

Peng, J., Liu, T., Huang, Y., Ling, Y., & Li, Z. (2021). *Satellite-Based Precipitation Datasets Evaluation Using Gauge Observation and Hydrological Modeling in a Typical Arid Land Watershed of Central Asia*.

Raval, M., Sivashanmugam, P., Pham, V., Gohel, H., & Kaushik, A. (2021). Automated predictive analytics tool for rainfall forecasting. *Scientific Reports*, 1–13. https://doi.org/10.1038/s41598-021-95735-8

Reza, M., Ali, M., Kamyab, T., Teymoori, J., & Brocca, L. (2021). *Regional Studies Evaluating three non-gauge-corrected satellite precipitation estimates by a regional gauge interpolated dataset over Iran*. *Journal of Hydrology : 38*(October). https://doi.org/10.1016/j.ejrh.2021.100942

Setegn, S. G., R. Srinivasan, A. M. Melesse, and B. Dargahi (2009a), *SWAT model application and prediction uncertainty analysis in the Lake Tana Basin*, Ethiopia, Hydrol. Processes, **23**, 3738– 3750.

Setiawati, M., & Miura, F. (2016). *Evaluation of GSMaP Daily Rainfall Satellite Data for Flood Monitoring*: Case Study, Kyushu Japan. Journal of Geoscience and Environment Protection, 4, 101. https://doi.org/10.4236/gep.2016.412008

Song, J. J., Innerst, M., Shin, K., Ye, B., Kim, M., Yeom, D., & Lee, G. (2021). *Estimation of Precipitation Area Using S-Band Dual-Polarization Radar Measurements*.

Tarnavsky, E., et al. (2014) *Extension of the TAMSAT Satellite-Based Rainfall Monitoring over Africa and from 1983 to Present*. Journal of Applied Meteorology and Climatology, 53, 2805-2822.

Teferi, M., Dyer, E., Charles, K. J., & Hirons, L. C. (2021). *Potential predictability of the Ethiopian summer rains : Understanding local variations and their implications for water management decisions.* Science of the Total Environment, *755*, 142604. https://doi.org/10.1016/j.scitotenv.2020.142604

Tian B. (2027). *GIS Technology Applications in Environmental and Earth Sciences*, Taylor & Francis Group, LLC, CRC Press is an imprint of Taylor & Francis Group, an Informa business.

Toté, C., Patricio, D., Boogaard, H., Wijngaart, R. Van Der, Tarnavsky, E., & Funk, C. (2015). *Evaluation of Satellite Rainfall Estimates for Drought and Flood Monitoring in Mozambique*. 1758–1776. https://doi.org/10.3390/rs70201758

Tramblay, Y., Thiemig, V., Dezetter, A., & Hanich, L. (2016). *Evaluation of satellite-based rainfall products for hydrological modelling in Morocco*. Hydrological Sciences Journal, *61*(14), 2509–2519. https://doi.org/10.1080/02626667.2016.1154149

Wang, Z., Zhong, R., Lai, C., & Chen, J. (2017). E*valuation of the GPM IMERG satellite-based precipitation products and the hydrological utility*. Atmospheric

Research, *196*(May), 151–163. https://doi.org/10.1016/j.atmosres.2017.06.020

World Bank (WB). (2019). *Disaster Risk profile: Ethiopia*. The World Bank group, 1818 H street, Washington, D.C. 20433, USA

World Meteorological organization (WMO). (2008). *Guide to Meteorological Instruments and Methods of Observation*. World Meteorological Organization, CH-1211 Geneva 2, Switzerland

Yared Bayissa, Tsegaye Tadesse, Getachew Demisse and Andualem Shiferaw. (2017). *Evaluation of Satellite-Based Rainfall Estimates and Application to Monitor Meteorological Drought for the Upper Blue Nile Basin, Ethiopia,* Remote Sens. **2017**, 9, 669; doi:10.3390/rs9070669

Yu, C., Hu, D., Liu, M., Wang, S., & Di, Y. (2020). S*patio-temporal accuracy evaluation of three high-resolution satellite precipitation products in China area*. Atmospheric Research, *241*(105), 104952. https://doi.org/10.1016/j.atmosres.2020.104952

Websites

http://www.ethiomet.gov.et/ accessed on 19/02/2022

https://www.chc.ucsb.edu/data accessed on 26/02/2022

http://www.TAMSAT-V3.1.org.uk/data/ accessed on 28/02/2022

https://chrsdata.eng.uci.edu/ accessed on 04/03/2022

Appendices

Annex1: Annual Rainfall

	Gauge					
Year	Debre Tabor	Wereta	Wanzaye	Agere Genet	Bahir Dar Airport	Bahir Dar New Station
2004	1198.1	1227.6	1088.7	800.7	1399.9	1399.9
2005	1486.9	1394.4	1197.5	1746.5	1382.1	1382.1
2006	1639.5	1508.4	1596.5	2000.3	1671.9	1671.9
2007	1542.6	1238	1463	1628.4	1956.7	1956.7
2008	1595.3	1602.3	1592.2	1912.5	1904.8	1904.8
2009	1234	1167.1	1370	1413.7	1070	1070
2010	1630.8	1455.7	1878.2	1906.2	1647.8	1647.8
2011	1533.2	1183.3	1306.4	2064.3	1676.7	1676.7
2012	1489.4	1241	1548.6	1644.3	1616.3	1616.3
2013	1673	1297.6	1442.9	1989.3	1828.6	1828.6
2014	1749.9	1233.4	1272.9	1783.6	1685.9	1685.9
2015	1202.6	2520.3	1238.2	1417.8	1283.1	1283.1
2016	1335.5		1492.1	1901.8	1324.4	1324.4
2017	1406	1088.5	1536.9	1239.9	1344.1	1344.1
2018	1609.5	1148.5	1473.1	2026.9	1464.4	1464.4
2019	1926.1	1279.1	1464.8	1536.7	1612.7	1612.7

Year	CHIRPS-V2					
	Debre Tabor	Wereta	Wanzaye	Agere Genet	Bahir Dar Air port	Bahir Dar new Station
2004	1241.76	1139.85	1184.91	1007.5	1219.18	1219.18
2005	1483.6	1279.18	1317.99	1213.27	1219.38	1219.38
2006	1777.36	1535.59	1664.17	1349.37	1622.5	1622.5
2007	1622.16	1328.36	1376.38	1332.79	1310.15	1310.15
2008	1680.31	1434.93	1490.79	1320.27	1517.46	1517.46
2009	1218.84	1101.31	1114.64	894.78	1093	1093
2010	1633.24	1376.97	1427.21	1270.04	1379.79	1379.79
2011	1610.92	1361.36	1423.82	1329.87	1372.33	1372.33
2012	1640.57	1412.22	1516.1	1256.37	1465.43	1465.43
2013	1770.72	1394.82	1461.38	1377.98	1497.24	1497.24
2014	1697.57	1296.75	1427.61	1391.98	1498.56	1498.56
2015	1483.14	1179.61	1255.68	1047.71	1201.09	1201.09
2016	1674.11	1352.48	1398.2	1365.1	1389.76	1389.76
2017	1753.37	1501.68	1554.28	1399.39	1616.68	1616.68
2018	1687.78	1323.74	1397.75	1339.73	1430.67	1430.67
2019	1973.13	1508.22	1636.81	1580.97	1563.51	1563.51

Year	PERSIANN-CDR					
	Debre Tabor	Wereta	Wanzaye	Agere Genet	Bahir Dar Airport	Bahir Dar New Station
2004	1082.91	1412.45	1412.45	930.43	1458.73	1458.73
2005	964	1100.76	1100.76	873.21	1174.82	1174.82
2006	1113.41	1534.09	1534.09	967.03	1609.63	1609.63
2007	1056.9	1230.1	1230.1	897.42	1181.75	1181.75
2008	1080.9	1505.73	1505.73	922.33	1539.65	1539.65
2009	784.46	965.33	965.33	665.38	929.8	929.8
2010	1066.87	1135.68	1135.68	1013.3	1145.85	1145.85
2011	932.01	1171.79	1171.79	812.62	1218.57	1218.57
2012	988.4	1122.73	1122.73	899.04	1226.12	1226.12
2013	955.38	1148.53	1148.53	852.59	1191.75	1191.75
2014	1082.91	1412.45	1412.45	930.43	1458.73	1458.73
2015	913.59	1280.3	1280.3	723.25	1337.79	1337.79
2016	976.67	1191.11	1191.11	828.22	1226.9	1226.9
2017	1015.52	1376.07	1376	944.71	1467.34	1467.34
2018	1092.8	1243.5	1243.5	1021.8	1412.52	1412.52
2019	1115.82	1408.92	1408.92	958.38	1443.72	1443.72

Year	TAMSAT-V3.1					
	Debre Tabor	Wereta	Wanzaye	Agere Genet	Bahir Dar Airport	Bahir Dar New Station
2004	1136.9	1028.3	1114.2	867.8	1213.6	1213.6
2005	1513.3	1316.5	1385.7	1137.9	1405	1405
2006	1582.9	1352.5	1468	1070.2	1485.9	1485.9
2007	1544	1283.5	1392.5	1299.3	1405.3	1405.3
2008	1633.5	1350.7	1494.8	1313.6	1537.2	1537.2
2009	1294.7	1055	1171.8	931.5	1161.2	1161.2
2010	1968.2	1601.6	1673.1	1506.3	1652.5	1652.5
2011	1519.2	1334.6	1413.5	1169.1	1404	1404
2012	1479.8	1327.5	1493.8	1214.8	1530.8	1530.8
2013	1631.6	1361.5	1462.7	1352.3	1406.2	1406.2
2014	1669.2	1297.1	1436	1387.6	1429.5	1429.5
2015	1532.5	1318.4	1448.2	1103.9	1385.4	1385.4
2016	1543	1311.4	1345.2	1276.2	1359.8	1359.8
2017	1653.2	1453.5	1527.7	1318.3	1575.4	1575.4
2018	1429.9	1249.9	1337.1	1188	1332.6	1332.6
2019	1604.3	1343.3	1486	1415.6	1473.9	1473.9

Annex 2: Kirmet Season Rainfall (2004-2019)

Year	**Gauge**						
	Debre Tabor	Wereta	Wanzaye	Agere Genet	BDR AP	Total	AV.
2004	890.7	1087.9	964.2	595	1225.7	4763.5	952.7
2005	1350.2	1256.8	1059.7	1556.3	1177.1	6400.1	1280.02
2006	1359.7	1184.9	1293.9	1573.7	1368.8	6781	1356.2
2007	1330.5	1171.5	1292.7	1273.8	1753.7	6822.2	1364.44
2008	1146.2	1137.9	1107.7	1468.4	1635.4	6495.6	1299.12
2009	1007.8	1089.2	1282	1133.7	991	5503.7	1100.74
2010	1397	779.3	1738.7	1562.1	1525.1	7002.2	1400.44
2011	1144.4	986	1064.6	1593.7	1424	6212.7	1242.54
2012	1328.7	1194	1460.4	1394	1559.4	6936.5	1387.3
2013	1242.3	1117.9	1263.3	1720.2	1539.2	6882.9	1376.58
2014	1181.8	1013.4	1069.5	1226.2	1276.3	5767.2	1153.44
2015	848	2157.3	885.8	995.8	956.9	5843.8	1168.76
2016	604.4		1196.9	1275.4	1209.5	4286.2	857.24
2017	991.7	914.2	1228.9	849.9	1171.3	5156	1031.2
2018	1378.2	1059.2	1212.9	1703.1	1205	6558.4	1311.68
2019	1482.8	1201.7	1194.4	1098.5	1248	6225.4	1245.08

	CHIRPS-V2						
	Debre Tabor	Wereta	Wanzaye	Agere Genet	BDR AP	Total	AV.
2004	1053.43	982.65	1016.11	794.2	1037.47	4883.86	976.772
2005	1109.71	1076.54	1114.75	1021.84	1039.56	5362.4	1072.48
2006	1299.78	1266.02	1320.29	1176.3	1278.17	6340.56	1268.112
2007	1150.72	1159.78	1156.09	1102.26	1065.46	5634.31	1126.862
2008	1152.94	1143.85	1195.72	1065.04	1152.41	5709.96	1141.992
2009	924.21	945.36	950.03	784.92	751.86	4356.38	871.276
2010	1198.34	1181.48	1214.2	1103.7	1161.99	5859.71	1171.942
2011	1096.63	1084.9	1008.25	1008.9	982.37	5181.05	1036.21
2012	1260.34	1267.29	1310.14	1137.57	1135.65	6110.99	1222.198
2013	1173.29	1133.74	1181.53	1071.43	1241.43	5801.42	1160.284
2014	1019.85	959.68	1069.54	886.53	1095.54	5031.14	1006.228
2015	930.64	911.63	957.14	786.09	947.99	4533.49	906.698
2016	1121.51	1049.06	1095.47	1117.09	1060.77	5443.9	1088.78
2017	1193.63	1210.98	1225.19	1077.8	1273.23	5980.83	1196.166
2018	1188.06	1115.86	1157.23	1102.63	1142.9	5706.68	1141.336
2019	1360.97	1226.08	1345.25	1217.55	1226.35	6376.2	1275.24

		TAMSAT-V3.1					
	Debre Tabor	Wereta	Wanzaye	Agere Genet	BDR AP	Total	AV.
2004	1083.96	937.4	1002	713	1058	4794.36	958.872
2005	1145.9	1011.3	1050.7	909.2	1239.9	5357	1071.4
2006	1293.9	1140.9	1224.5	836.3	1193.7	5689.3	1137.86
2007	1293	1154.2	1216	1071.1	1152.5	5886.8	1177.36
2008	1297.8	1145.3	1250.4	957.2	1287.8	5938.5	1187.7
2009	1139.2	995.6	1077.3	768.3	1070.4	5050.8	1010.16
2010	1749.5	1480.6	1550.8	1326.6	1489.6	7597.1	1519.42
2011	1261.5	1153.3	1211.2	924.4	1213.1	5763.5	1152.7
2012	1352.1	1220.3	1362.6	1048.2	1375.9	6359.1	1271.82
2013	1377.4	1166.8	1249.5	1053.8	1190.9	6038.4	1207.68
2014	1129.4	998	1070.2	817	1069.2	5083.8	1016.76
2015	1238.5	1075.8	1182.1	821.6	1104.7	5422.7	1084.54
2016	1263.1	1091.1	1152.9	958.6	1091.8	5557.5	1111.5
2017	1430.2	1282.2	1324.5	1069.6	1319	6425.5	1285.1
2018	1223.2	1083.8	1165.1	980	1133.5	5585.6	1117.12
2019	1194.2	1099.3	1217.1	934.7	1208.2	5653.5	1130.7

	PERSIANN-CDR- CDR						
	Debre Tabor	Wereta	Wanzaye	Agere Genet	BDR AP	Total	AV.
2004	686.31	936.12	936.2	616.38	1022.38	4197.39	839.478
2005	700.44	838.61	838.609	634.97	899.19	3911.819	782.3638
2006	771.2	1078.44	1078.44	712.51	1139.65	4780.24	956.048
2007	740.67	995.13	995.13	683.33	921.22	4335.48	867.096
2008	611.41	906.03	906.03	558.7	1009.63	3991.8	798.36
2009	514.09	780.31	780.31	479.65	775.59	3329.95	665.99
2010	885.78	1075.56	1075.56	877.54	1100.76	5015.2	1003.04
2011	624.47	871.86	871.86	560.51	919.09	3847.79	769.558
2012	720.97	839.81	831.89	682.66	874.23	3949.56	789.912
2013	686.37	825.8	825.8	656.73	829.99	3824.69	764.938
2014	660.81	854.93	854.93	635.01	928.11	3933.79	786.758
2015	562.48	878.38	878.38	492.15	940.93	3752.32	750.464
2016	652.48	791.69	791.69	597.86	833.85	3667.57	733.514
2017	612.32	937.63	937.63	605.78	970.61	4063.97	812.794
2018	793.33	999.34	999.34	763.82	1099.75	4655.58	931.116
2019	618.73	978.56	979.56	551.04	1032.52	4160.41	832.082

Annex 3: Monthly Rainfall (2004-2019)

Year	Month	**Gauge**				
		Debre Tabor	Wereta	Wanzaye	Agere Genet	BDR AP
2004	June	141	163.1	117.9	104.8	150.2
	July	333.7	382.1	378.8	406.4	458
	August	25.2	410.2	256.4		410.9
	September	120.8	132.5	211.1	83.8	206.6
2005	June	224.4	262.1	136.8	47.5	141.8
	July	472.6	261.8	334.1	628.1	496.7
	August	436	461.6	289	577.3	292
	September	216.2	271.3	299.8	303.4	246.4
2006	June	170	118.9	52	167.7	196.8
	July	482.2	388.7	413.1	695.5	583.1
	August	452.5	497	599.4	570.4	394
	September	255	180.3	199.4	140.1	194.9
2007	June	271.2	167.5	301.9	300.3	315.4
	July	425.7	232.3	344	477.3	744
	August	439.1	425	393	329.3	407.7
	September	194.5	346.7	253.8	166.9	286.3
2008	June	209.4	151.7	177	264.4	292.8
	July	376.4	395.7	391.2	394.3	725.5
	August	331.8	433	386.2	556.7	407.5
	September	228.6	157.5	153.3	253	209.6
2009	June	66.8	121.8	103.1	59.4	59.5
	July	408.3	451.5	436.4	500.8	419.3
	August	410.5	356.5	658.6	429.7	434.7
	September	122.2	159.4	83.9	143.8	77.5
2010	June	166.8	426.6	225.8	85.3	129.9
	July	499.3	291.5	460.6	515.5	407.8
	August	527.9	61.2	739.9	730.8	449.3
	September	203	0	312.4	230.5	182.2
2011	June	132.9	71.7		152.5	257.4
	July	359.6	424.1	396.9	773.2	529.1
	August	392.2	331.9	406.9	475.3	394.6
	September	259.7	158.3	260.8	192.7	242.9
2012	June	277.7	172.3	134.9	150.8	184.2
	July	389.3	382.9	481.7	622.1	515.9
	August	447.7	392.7	400.3	396.2	524.9
	September	214	246.1	443.5	224.9	334.4

2013	June	248.9	221.4	145.9	230.3	206.5
	July	423	354.5	556.9	725.1	765
	August	439.1	383.2	372.9	661	460.6
	September	131.3	158.8	187.6	103.5	107.1
2014	June	165.2	86.6	255.8	62.5	169.6
	July	340.8	283.9	295.3	390.2	356.6
	August	453.6	424.4	301.4	550.5	502.2
	September	222.2	218.5	217	223	247.9
2015	June	129.2	184.5	103.1	136.1	137.7
	July	234.1	759.6	264.9	173.7	383
	August	284.2	1015.4	364.1	458	266.1
	September	200.5	197.8	153.7	228	170.1
2016	June	398.8		226.3	93.8	224.4
	July	177.9		446.1	630.2	462.5
	August	27.9		346.8	393.3	281.2
	September	0		177.7	158.1	241.4
2017	June	84.4	50.6	161	6.9	78.8
	July	346	346.8	545	250.8	502.5
	August	276.3	404.3	359.6	487.5	400.5
	September	285	112.6	163.3	104.7	189.5
2018	June	304	227.7	230.3	216.3	227.7
	July	440.2	486.3	429.8	570.3	410
	August	422.7	323.6	405.2	629.4	376.4
	September	211.3	21.3	147.6	287.1	190.9
2019	June	226	162.1	294.3	78.5	378.4
	July	385.5	458	329	446.8	353.6
	August	564	342.5	391.2	573.2	276.9
	September	307.3	239.1	179.9		239.1

Year	Month	CHIRPS-V2				
		Debre Tabor	Wereta	Wanzaye	Agere Genet	BDR AP
2004	June	153.58	145.61	144.17	101.38	153.22
	July	417.52	384.45	391.23	325.84	407.06
	August	358.13	299.21	290.75	272.47	280.23
	September	124.2	153.38	189.96	94.51	196.96
2005	June	137.89	167.46	154.43	121.48	194.79
	July	398.77	387.62	379.11	409.41	345.64
	August	335.41	319.81	316.92	321.72	292.62
	September	237.64	201.66	264.30	169.24	206.52
2006	June	161.98	182.29	197.33	122.10	250.89
	July	430.35	430.52	422.73	427.91	416.27
	August	446.12	412.17	414.73	434.33	393.28
	September	261.34	241.05	285.51	191.96	217.73
2007	June	192.08	269.23	241.79	192.84	276.88
	July	394.77	362.17	361.62	379.28	314.44
	August	355.50	353.76	333.95	341.21	292.01
	September	208.38	174.62	218.74	188.94	182.14
2008	June	172.14	214.18	202.65	142.62	218.73
	July	391.69	390.95	394.52	376.90	375.69
	August	382.29	357.26	375.56	362.16	347.78
	September	206.83	181.46	223.00	183.37	210.22
2009	June	111.79	154.62	141.45	73.27	215.70
	July	380.15	385.59	359.80	358.03	119.48
	August	314.98	311.18	317.59	269.42	297.11
	September	117.29	93.98	131.20	84.20	119.57
2010	June	97.68	132.57	124.47	69.08	195.68
	July	447.71	431.60	428.59	448.44	393.76
	August	439.34	434.00	409.97	430.43	328.21
	September	213.61	183.31	251.18	155.74	244.35
2011	June	138.24	173.71	158.42	109.65	190.60
	July	387.86	380.72	372.41	383.65	344.68
	August	369.37	343.93	361.58	332.01	287.61
	September	201.16	185.72	215.84	183.60	159.49
2012	June	189.42	214.63	211.69	153.66	222.15
	July	425.45	441.61	424.10	451.18	338.77
	August	390.10	386.31	397.57	356.72	359.22
	September	255.88	224.74	276.78	176.01	215.51
2013	June	155.61	179.59	176.46	135.13	212.75
	July	467.87	484.67	476.58	440.63	521.45

	August	399.37	350.12	363.53	377.71	349.66
	September	150.45	119.35	164.95	117.95	157.57
2014	June	126.37	139.45	151.76	89.26	191.25
	July	318.72	306.56	322.26	299.35	340.52
	August	323.44	304.84	306.60	311.82	284.31
	September	251.32	208.83	288.92	186.10	279.46
2015	June	97.27	106.82	110.48	82.00	139.37
	July	253.63	281.67	268.04	210.83	277.95
	August	320.03	300.61	303.66	297.15	272.82
	September	259.71	222.54	274.96	196.12	257.85
2016	June	121.78	138.75	138.68	126.55	181.71
	July	459.88	429.75	440.04	467.94	395.85
	August	382.75	341.05	337.04	397.69	293.64
	September	157.10	139.51	179.71	124.92	189.57
2017	June	98.64	131.50	117.02	75.32	152.56
	July	440.72	445.78	454.18	386.97	467.79
	August	434.78	430.46	400.52	450.92	366.38
	September	219.49	203.23	253.47	164.60	286.49
2018	June	204.75	244.12	219.57	187.61	228.32
	July	391.39	354.76	369.14	378.12	370.57
	August	371.59	346.50	345.53	359.46	317.89
	September	220.33	170.48	223.00	177.46	225.31
2019	June	279.82	285.76	300.84	238.91	299.37
	July	362.95	331.84	359.99	331.07	355.28
	August	345.21	318.39	322.11	326.64	303.74
	September	373.00	290.10	362.31	320.93	267.96

Year	Month	TAMSAT-V3.1				
		Debre Tabor	Wereta	Wanzaye	Agere Genet	BDR AP
2004	June	196.96	109.2	107.2	75.1	113.6
	July	414.6	405.2	427.1	290.6	453.6
	August	393.2	305.5	326.5	281.1	326.7
	September	79.2	117.5	141.2	66.2	164.1
2005	June	152.3	172.1	159.2	81.8	170.9
	July	555.9	467.7	458.9	394.5	442.9
	August	430.7	365.2	380.4	338.3	387.1
	September	159.3	178.4	211.4	94.6	239
2006	June	169	169.5	194.7	44.1	210.3
	July	390.4	342.7	341.4	274.8	366.3
	August	575.2	445.1	459.8	425.9	403.5
	September	159.3	183.6	228.6	91.5	213.6
2007	June	202.3	217.7	222.3	164	224.7
	July	517.2	412	426.9	456.5	370.8
	August	416.1	377.4	380.8	314.9	357.2
	September	157.4	147.1	186	135.7	199.8
2008	June	187.4	184.6	197.4	107.8	201.7
	July	485.2	412.1	437.7	362.4	460.3
	August	458	382.1	427.6	344.8	431.8
	September	167.2	166.5	187.7	142.2	194
2009	June	210.7	194.8	214.3	107.1	208.2
	July	467.2	387.6	397.6	329.8	367.3
	August	385.5	329.6	361.6	286.4	367.5
	September	75.8	83.6	103.8	45	127.4
2010	June	156.7	140.9	155.9	98.6	186.7
	July	700.6	591.3	598.5	538.7	572.8
	August	743.9	578.7	595.3	587.5	526.3
	September	148.3	169.7	201.1	101.8	203.8
2011	June	180.4	196.7	209.9	110.2	240.1
	July	494.5	426.6	423.2	376	407.8
	August	477.2	401.3	421.8	360.9	399.6
	September	109.4	128.7	156.3	77.3	165.6
2012	June	148.6	161.1	175.6	106.6	189.6
	July	636.3	532.3	564.6	507.1	571.3
	August	404.1	332.6	375	318.7	380.3
	September	163.1	194.3	247.4	115.8	234.7
2013	June	123.6	118.1	130.7	72.1	121.3
	July	673.8	566	592.5	519	572.2

	August	470	369.4	378	356.6	341.4
	September	110	113.3	148.3	106.1	156
2014	June	85	109.9	124.5	42	145.8
	July	347.3	298.6	300.7	253.4	326
	August	496.5	397.7	418.3	375.9	359.7
	September	200.6	191.8	226.7	145.7	237.7
2015	June	105.1	101.1	111.1	60.3	127.2
	July	437.9	378.8	439.5	251.7	394.6
	August	465.7	380.6	392.7	338.8	351.4
	September	229.8	215.3	238.8	170.8	231.5
2016	June	148.1	135.3	163.8	112.3	181.6
	July	553.9	485.5	487.4	441.1	456.6
	August	452.5	342.8	365.1	324.7	326.3
	September	108.6	127.5	136.6	80.5	127.3
2017	June	88.2	126	120.6	34.7	129.7
	July	555.2	475.3	488.8	418.3	529.9
	August	645.2	521.6	519.6	489.2	451.4
	September	141.6	159.3	195.5	127.4	208
2018	June	184.2	200	217.7	122.3	205.1
	July	407	330.1	352.6	329.9	364.4
	August	411.2	343.5	347.5	336.1	327.9
	September	220.8	210.2	247.3	191.7	236.1
2019	June	203.2	207.3	230.5	145.8	246.2
	July	410.7	371.7	402.1	304.6	397.6
	August	348.4	296.2	321.8	262.4	324.3
	September	231.9	224.1	262.7	221.9	240.1

Year	Month	PERSIANN-CDR				
		Debre Tabor	Wereta	Wanzaye	Agere Genet	BDR AP
2004	June	115.62	125.38	125.38	105.98	149.04
	July	239.43	337.19	337.19	222.08	400.53
	August	260.35	306.89	306.89	237.18	312.16
	September	70.91	166.66	166.66	51.14	160.65
2005	June	69.26	110.91	110.91	41.59	145.91
	July	315.46	306.75	306.759	301.01	303.67
	August	223.48	276.44	276.43	228.64	295.55
	September	92.24	144.51	144.51	63.73	154.06
2006	June	50.49	213.36	213.36	26.55	223.34
	July	304.04	344.31	344.31	294.04	421.03
	August	317.8	312.77	312.77	319.87	325.69
	September	98.87	208	208	72.05	169.59
2007	June	112.05	232.17	232.17	62.58	203.36
	July	325.48	333.98	333.98	314.66	292.28
	August	224.32	287.38	287.38	226.69	283.4
	September	78.82	141.6	141.6	79.4	142.18
2008	June	35.81	108.25	108.25	21.3	146.72
	July	237.24	332.47	332.47	226.11	373.16
	August	262.06	348.11	348.11	239.69	366.39
	September	76.3	117.2	117.2	71.6	123.36
2009	June	46.33	97.41	97.41	23.98	106.83
	July	215.91	349.41	349.41	219.18	345.16
	August	201.37	258.11	258.11	203.52	258.99
	September	50.48	75.38	75.38	32.97	64.61
2010	June	99.29	271.44	271.44	71.96	310.18
	July	308.64	282.25	282.25	301.49	277.53
	August	393.44	373.97	373.97	438.12	348.42
	September	84.41	147.9	147.9	65.97	164.63
2011	June	67.53	131.92	131.92	41.74	179.1
	July	204.54	270.97	270.97	171	256.69
	August	277.33	315.43	315.43	295.26	315.71
	September	75.07	153.54	153.54	52.51	167.59
2012	June	29.16	60.26	60.26	19.51	64.61
	July	274.1	249.61	241.69	311.19	285.97
	August	279.25	294.17	294.17	255.59	289.71
	September	138.46	235.77	235.77	96.37	233.94
2013	June	39.12	102.36	102.36	28.24	102.58
	July	298.1	329.62	329.62	302.53	356.88

	August	286.21	275.63	275.63	279.55	283.28
	September	62.94	118.19	118.19	46.41	87.25
2014	June	33.4	126.82	126.82	17.44	156.94
	July	228.74	255.44	255.44	226.23	261.2
	August	272.47	300.42	300.42	280.26	331.71
	September	126.2	172.25	172.25	111.08	178.26
2015	June	36.62	80.5	80.5	21.51	101.93
	July	141.77	352.5	352.5	116.45	371.73
	August	250.26	262.28	262.28	231.67	285.47
	September	133.83	183.1	183.1	122.52	181.8
2016	June	55.76	141.29	141.29	44.46	184.81
	July	267.53	274.01	274.01	238.31	290.22
	August	266.11	281.67	281.67	268.6	247.69
	September	63.08	94.72	94.72	46.49	111.13
2017	June	34.19	89.95	89.95	21.45	78.29
	July	202.26	327.87	327.87	195.56	344.59
	August	277.67	331.5	331.5	298.18	331.08
	September	98.2	188.31	188.31	90.59	216.65
2018	June	97.69	195.85	195.85	72.03	197.72
	July	263.19	316.8	316.8	267.3	388.42
	August	286.18	297.57	297.57	294.56	333.06
	September	146.27	189.12	189.12	129.93	180.55
2019	June	116.89	265.3	265.3	73.01	286.85
	July	173.87	242.79	242.79	162.97	258.58
	August	166.09	231.6	231.6	172.37	260.65
	September	161.88	238.87	239.87	142.69	226.44